Fracture In A Plate Girder Railway Bridge

Joseph Schneider

A Major Technical Report

in

The Department

of

Civil Engineering

Presented in Partial Fulfillment of the Requirements
for the Degree of Master of Engineering at
Concordia University
Montréal, Québec, Canada

June 1986

ISBN 0-315-32236-5

ABSTRACT

Failure In A Plate Girder Railway Bridge

Joseph Schneider

A large crack was discovered in June 1976 in a plate girder railway bridge. Fatigue cracks originated in the partial penetration weld of a horizontal stiffener and penetrated the girder web, resulting in a 1.25 metre long crack.

Analytical studies were carried out to determine the theoretical life of the welded detail and the results are compared with the life of the actual detail that suffered failure. Retrofit procedures are described and evaluated through a field inspection performed in October 1985, nine years after the retrofitting.

Conclusions are drawn from the analysis and inspection of the retrofits and presented as recommendations for future design of similar details.

ACKNOWLEDGEMENTS

This paper would not have been completed without the assistance and support of many people and a number of companies.

Accordingly the author wishes to thank the following:

- Canadian Pacific Limited for their permission to examine and discuss the failure,
- AMCA International Limited (formerly Dominion Bridge Co Ltd) for providing copies of the original fabrication drawings and design briefs of the bridge,
- Dr. M.S. Troitsky for his patience, supervision and support during the development of this paper,
- Dr. K. Ghavami for his critical review and constructive comments,
- The Schneider family for their persistence in prodding the author to continue,
- Hilary Barton for her efficient and expert typing of the manuscript.

TABLE OF CONTENTS

NOTATIONS

- a - width of hole parallel to the applied stress
- A - area
- b - width of hole perpendicular to the applied stress
- C - influence line coefficient
- d - the number of standard deviations below the mean-line
- f - unit stress
- f_g - unit stress on gross area
- f_n - unit stress on net area
- h - height
- I - moment of inertia
- I_v - vertical impact factor percent
- I_{xx} - moment of inertia about the xx axis
- K_o - constant term relating to the mean-line of statistical analysis results
- K_{tn} - stress concentration factor based on the net area stress
- K_∞ - stress concentration factor in an infinitely wide plate
- L - length
- m - the inverse slope of the mean-line log σ_r - log N curve
- M - bending moment
- n - number of cycles
- N - number of cycles to failure
- P - load
- SCF - stress concentration factor
- t_g - gross thickness

t_n - net thickness

w - width of plate

y - distance from the neutral axis

Δ - the reciprocal of the anti-log of the standard deviation of log N

σ - the non-propagating stress range for $N = 10^7$ cycles

σ_r - stress range

LIST OF FIGURES

LIST OF TABLES

CHAPTER 1

GENERAL INTRODUCTION

1.1 Introduction

During the first half of this century the design of railway bridges did not change appreciably, except for the trend to somewhat heavier live loading and the appearance and use of marginally higher yield steel. In the area of fabrication, rivetting remained the predominant method of fastening and details that had proved to be suitable through experience were copied repeatedly.

As a result, fatigue failures were relatively rare and this can be attributed to the following:

(a) The use of lower yield strength material resulted in less available stress for live load. As a consequence the stress range, one of the significant components in fatigue, was also low.

(b) The transportation explosion for moving goods both within Canada and for export had not yet occurred. Therefore the number of cycles experienced within any period was also low.

(c) Rivetting provided excellent fatigue resistant details, as later research would show. Furthermore, the rivet holes had an additional beneficial feature as they acted as crack arresters, should some failure occur, thus preventing or significantly delaying the appearance of large cracks.

By the 1960's the railways accepted the "modern" fabrication approaches and made the switch to welded construction. Unfortunately

the early welded designs incorporated details patterned after the existing rivetted construction details, instead of developing new details more suitable to welding and welded design.

This switch to welding together with heavier average loading caused by the need to be more competitive in the transporting of raw materials and manufactured goods, the increased frequency of travel resulting from the transportation explosion and the higher live load stress range available from the use of higher yield strength steel resulted in a significant increase of fatigue related failures.

1.2 Objectives

The primary objectives of this report are:

(a) to investigate and analyse a specific bridge girder failure

(b) to evaluate the effectiveness of the retrofits provided

(c) to make recommendations for future designs that would prevent the recurrence of similar failures.

1.3 Outline of The Report

Chapter 2 presents a description of the structure and the loading history prior to the discovery of the failure.

Chapter 3 presents a detailed description of the failures found. Both the major failure, the main subject of this report and other

minor failures are described.

Chapter 4 presents the analysis developed to determine, from a theoretical basis, the expected life of the failed detail. The analysis uses the most current guidelines available for evaluating low stress cycles and variable loading effects in the calculation of fatigue life.

Chapter 5 presents a description of the progressive stages of the failure from the initial crack initiation through to the final full failure pattern.

Chapter 6 outlines the methods used for retrofitting the different elements at the failure locations.

Chapter 7 presents an evaluation of the effectiveness of the retrofitting. The basis of this evaluation is an inspection carried out nine (9) years after the retrofitting work was completed.

Chapter 8 presents the conclusions drawn from the previous chapters and offers design and fabrication recommendations to prevent similar failures in future designs.

CHAPTER 2

DESCRIPTION OF THE STRUCTURE

2.1 Introduction

Bridge 8.75 spans across and over Ontario Highway 7 approximately five (5) kilometres west of the City of Ottawa in the vicinity of Bells Corners. The bridge is on a straight portion of the railway line and therefore no centrifugal forces occur during the passage of a train.

In this chapter the bridge geometry is described, the splicing of the horizontal stiffener is examined and the loading history of the bridge, prior to the discovery of the failure, is examined.

2.2 Bridge Geometry

The structure is a four span continuous bridge with spans measuring 28.651 m, 35.814 m, 35.814 m and 28.651 m. The bridge is also severely skewed with a skew angle of 66 degrees from normal, all as shown in Fig. 1.

The cross-section of the bridge, shown in Fig. 2, consists of two welded through plate girders (TPG) spaced 5.410 m centre-to-centre and carries a single track located on the longitudinal centre-line of the span.

The girders are 2.743 m deep, shop welded in lengths of between 16.750 m and 20.750 m. Each girder has continuous horizontal stiffeners

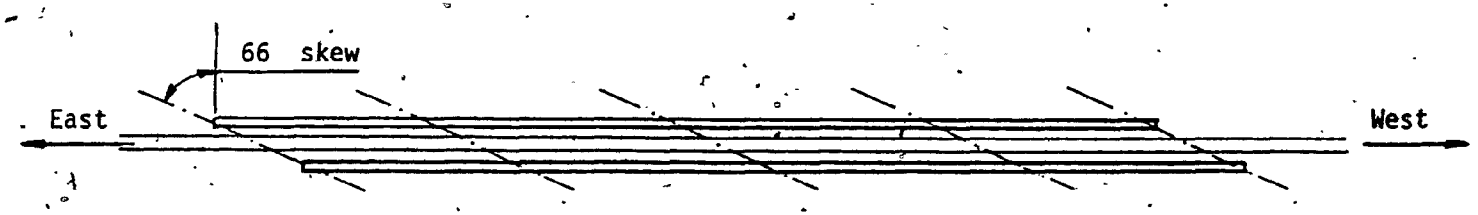

PLAN

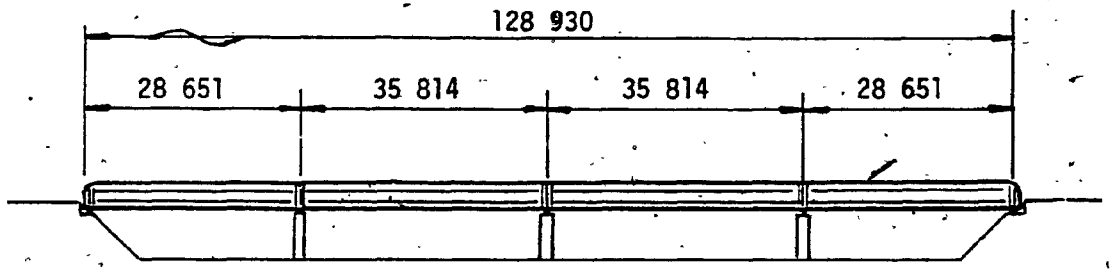

ELEVATION

FIG. 2.1 - BRIDGE 8.75 - PLAN and ELEVATION

welded to the exterior face of the web at a distance of 0.2h or 0.546 m from the top and bottom flanges. Vertical stiffeners are welded to the web on the interior face, spaced at approximately 1.2 m. The shop welded girders are made continuous by field bolted splices.

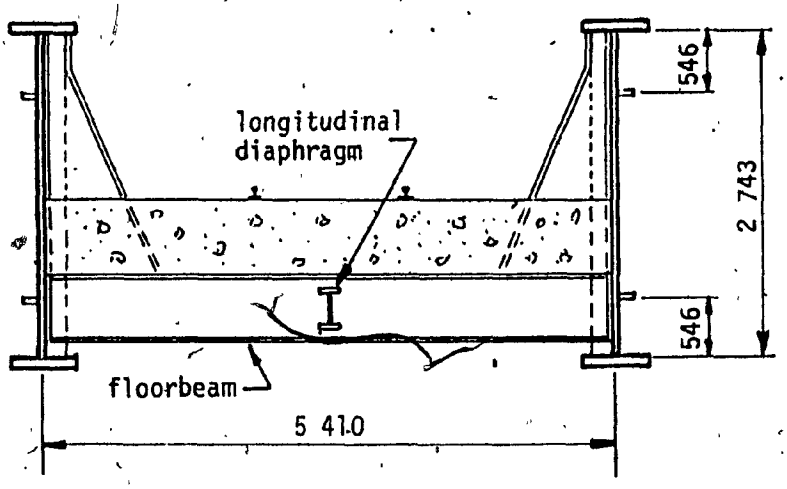

FIG. 2.2 - BRIDGE 8.75 - TYPICAL CROSS-SECTION

The floor system consists of W 610x140 transverse floorbeams. The floorbeams are at right angle to the longitudinal centre-line spaced at approximately 1.25 m for the full length of the bridge. A single longitudinal diaphragm is located between the floorbeams on the centre-line.

The rails are supported directly on a 1.0 m concrete ballasted deck which was poured in situ over the top of the floor system.

2.3 Detail of Horizontal Stiffener Weld

The shop weld, splicing the horizontal stiffeners, was a partial penetration weld as shown in Fig. 2.3. The outside surfaces of the weld were ground flush, leaving a net total throat of 5 mm based on measurements taken after the failure.

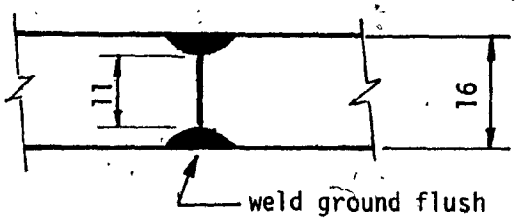

FIG. 2.3 - PARTIAL PENETRATION STIFFENER WELD

2.4 Loading History

The failure was discovered in June 1976 at which time the structure had been in service for about ten (10) years. Based on information from the railway, the traffic over that period consisted of light passenger trains and the occasional emergency rerouting of light freight trains.

The light passenger trains were made up of one electric locomotive followed by four passenger cars, as an average. The frequency of travel over the ten years was two trains per day in each direction. The typical VIA passenger train and its loading pattern is shown in Fig. 2.4.

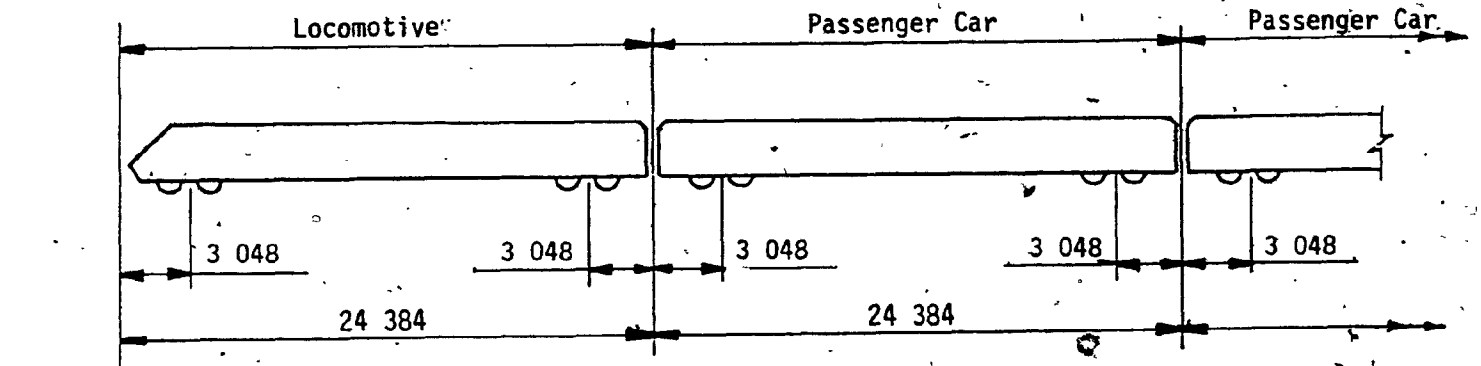

TYPICAL TRAIN

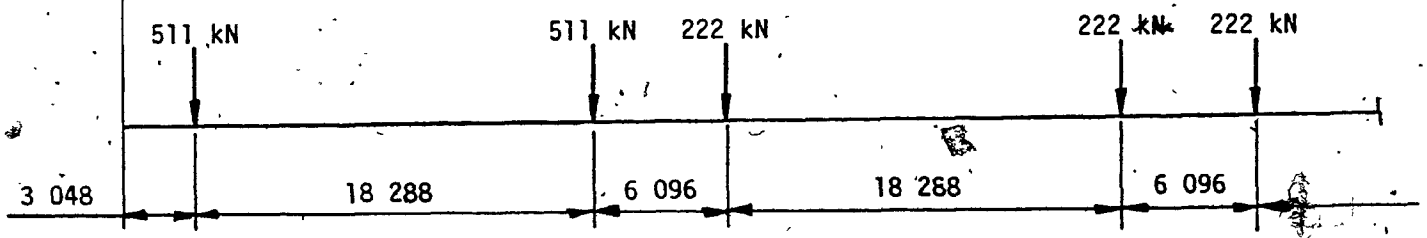

TYPICAL LOADING

FIG. 2.4 - VIA TRAIN - DIMENSIONS and LOADING

The emergency fright, for the purposes of this work, was assumed to be equivalent to a Cooper E50 loading made up of one locomotive followed by fifty (50) freight cars. The frequency of this loading over the ten years was assumed to be one train per month. The assumed emergency freight and its loading pattern is shown in Fig. 2.5.

All the above information on loading and frequency of travel is summarized in Table 2.1

YEARS of SERVICE	10
PASSENGER TRAINS per YEAR	1460
PASSENGER LOCOMOTIVES per TRAIN	1
PASSENGER LOCOMOTIVE LOAD	1022 kN
PASSENGER CARS per TRAIN	4
PASSENGER CAR LOAD	444 kN
FREIGHT TRAINS per YEAR	12
FREIGHT LOCOMOTIVES per TRAIN	1
FREIGHT LOCOMOTIVE LOAD	1580 kN
FREIGHT CARS per TRAIN	50
FREIGHT CAR LOAD	1776 kN

TABLE 2.1 - LOADING HISTORY

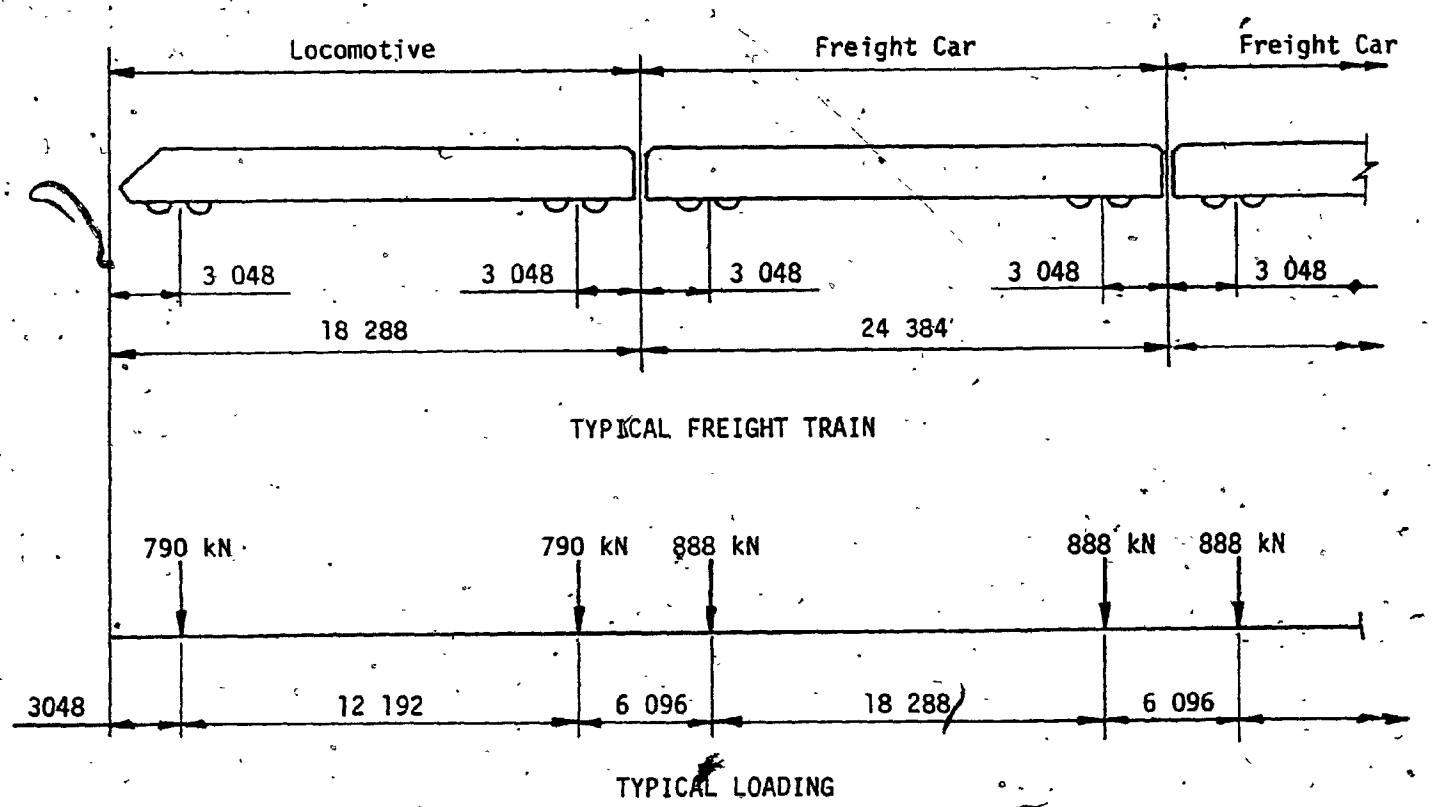

FIG. 2.5 - FREIGHT TRAIN - DIMENSIONS and LOADING

CHAPTER 3

DESCRIPTION OF THE FAILURE

3.1 Introduction

In this chapter the three failures that were discovered in the various bridge elements are described.

These are classified as:

(a) Minor Failures - where the crack had initiated in a secondary element but had not propagated into any main material

(b) Major Failure - where the crack had propagated from the secondary element and progressed into or through the main material

3.2 Minor Failures

Two locations on the bridge were discovered to have minor failures. These locations are shown in Fig. 3.1, and both failures occurred in the north girder.

In both instances the cracks coincided with a shop welded splice in the horizontal stiffener. At these locations the stiffener had not separated nor had the crack tip extended into the main web material. At both locations the crack was not visible as the paint film had not separated. However, when the paint was removed the crack was visible even to the naked eye. Examination with magnetic

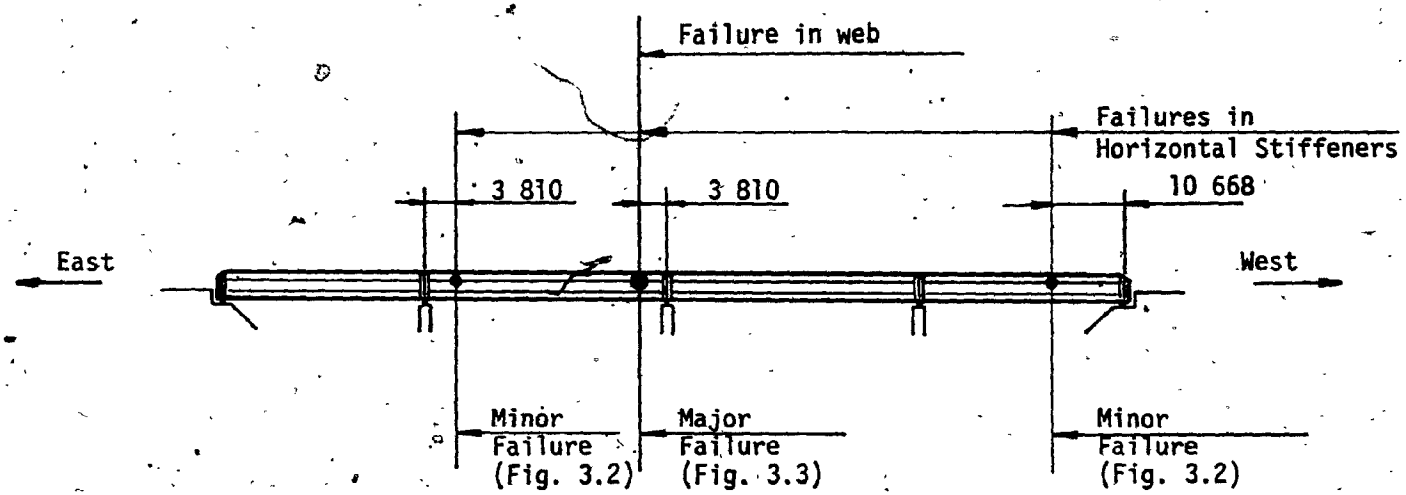

Outside Elevation

FIG. 3.1 - FAILURE LOCATIONS (NORTH GIRDER)

partical testing equipment revealed that the crack, in both instances, was on the face nearer the top flange of the girder. An enlarged detail of the minor failures is shown in Fig. 3.2.

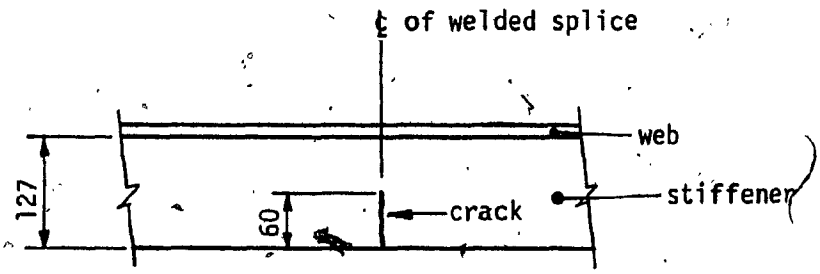

Plan View of Stiffener

FIG. 3.2 - MINOR FAILURES (ENLARGED DETAIL)

3.3 Major Failure

Also shown in Fig. 3.1 is the location of the major failure in the bridge. This large crack was found in the north girder approximately 3.8 m east of the centre pier.

The horizontal stiffener at the failure location had fractured and was totally separated. The failure in the stiffener occurred at a location similar to the minor failures, at a shop welded splice. The fracture had also penetrated the full thickness of the main web material. Web separation had occurred and took the form of an elongated "S", extending above and below the horizontal stiffener with a

total length of 1.25 m.

The crack, at the top, stopped 60 mm from the top flange to web fillet weld toe and, at the bottom, 45 mm above the level of the concrete ballast deck. An enlarged view of the major failure is shown in Fig. 3.3.

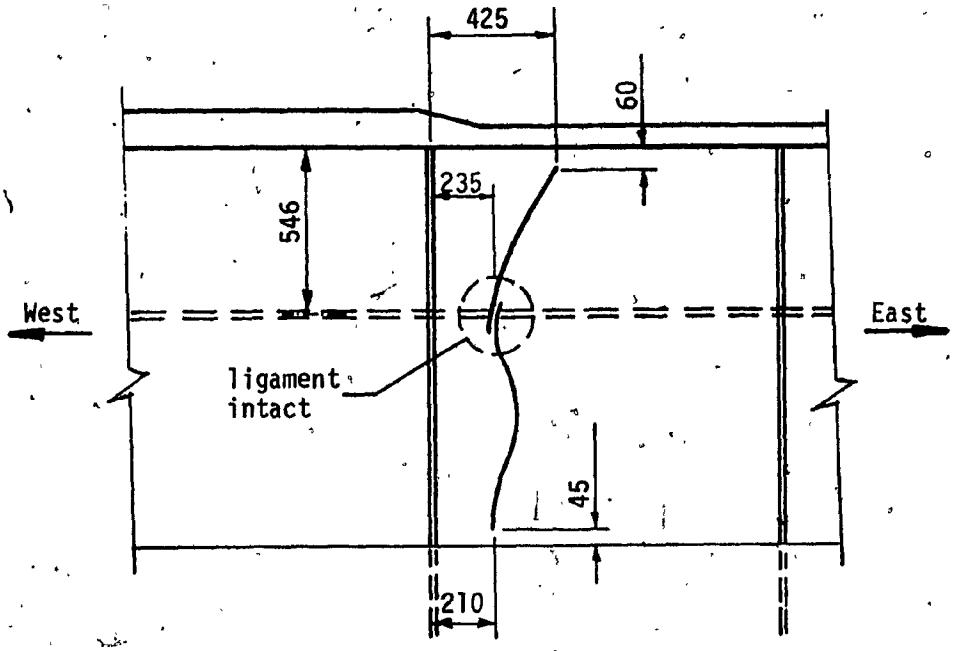

Inside Elevation

FIG. 3.3 - MAJOR FAILURE (ENLARGED DETAIL)

3.3.1 Examination of Major Failure

A close examination of the web failure, opposite the horizontal stiffener, revealed a thin ligament of web that had not separated. This intact piece of web provided the evidence that two cracks entered the web. The crack from the top surface of the partial penetration weld in the horizontal stiffener penetrated the web on the left side, as shown in Fig. 3.3, and progressed upward toward the top flange while the crack from the bottom surface of the stiffener weld penetrated the web on the right side and progressed downward toward the bottom flange. Both cracks, after penetrating the web, followed a path normal to the direction of the principal stress.

From these observations it was concluded that the failure was due to fatigue from repeated dynamic loading rather than a simple overload.

CHAPTER 4

ANALYSIS OF THE MAJOR FAILURE

4.1 Introduction

Bridge structures, such as the one being examined, are designed on the basis that each element functions independently. However, when the bridge is in service, all elements function together with the result that some elements, considered redundant in the initial design, are subjected to significant stresses by virtue of their participation in the overall scheme of load distribution.

This chapter analyses the major failure which was found to originate in the horizontal stiffener, an element generally considered to be redundant in many designs but subjected to significant participating stresses with the passage of live loads.

The factors considered are:

(a) the assessment of multiple cycles from the passage of a single train

(b) the stress concentration due to the partial penetration weld

(c) the effect of variable amplitude stresses

(d) the assessment of low stress cycles

The method used to evaluate the fatigue life is as outlined in

British Standard BS 5400 : 1980 : Part 10 [1]. The approach uses a cumulative damage evaluation, generally referred to as The Palmgren-Miner Rule. Since the investigation is of an actual failure, a higher probability of failure is also included in the determination of the total fatigue life. In addition, the effects of low stress cycles, those below the non-propagating stress level for constant amplitude fatigue life, are included in the calculations through the use of an adjusted slope of the σ_r - N curve.

4.2 Moment Range History - Passenger Train

Data for calculating the moment range history of a typical passenger train was gathered by traversing, mathematically, one passenger train across the major failure point influence line shown in Fig. 4.1

By moving the train incrementally, in one-tenth span increments, across the influence line a continuous moment history spectrum was determined at the failure location from the passing of one passenger train. The moment history spectrum is plotted in Fig. 4.2.

Calculations of the moment ranges from this history spectrum was accomplished by using the 'reservoir' method of cycle counting described in detail in BS 5400 : 1980 : Part 10 : Appendix 'B'. The 'reservoir' method provides a means of reducing an irregular series of stress fluctuations to a simple list of stress ranges. This method is suitable when dealing with short stress histories, such as those produced by individual loading events. It consists of imagining a plot of the graph of each individual stress history

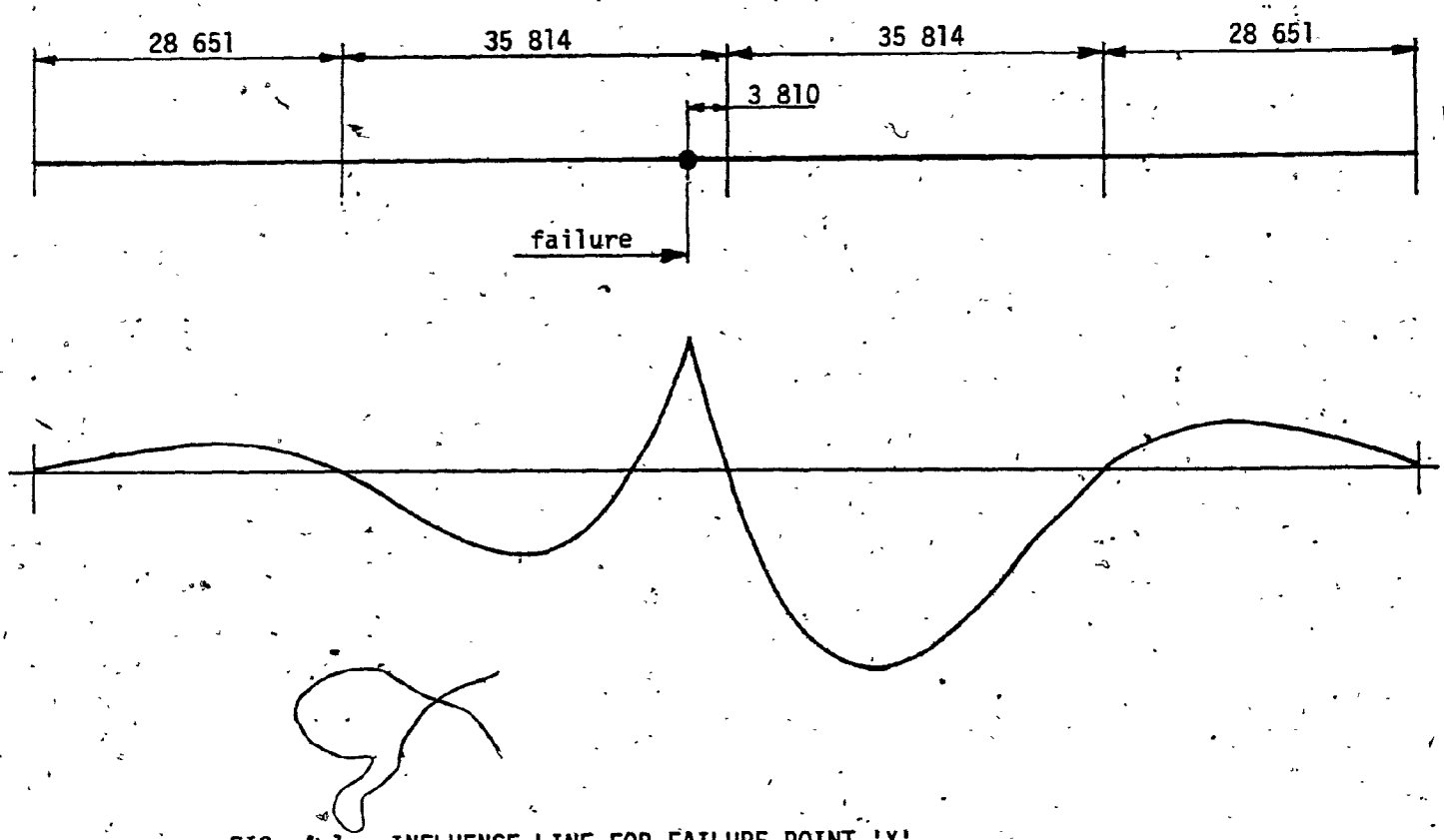

FIG. 4.1 - INFLUENCE LINE FOR FAILURE POINT 'X'

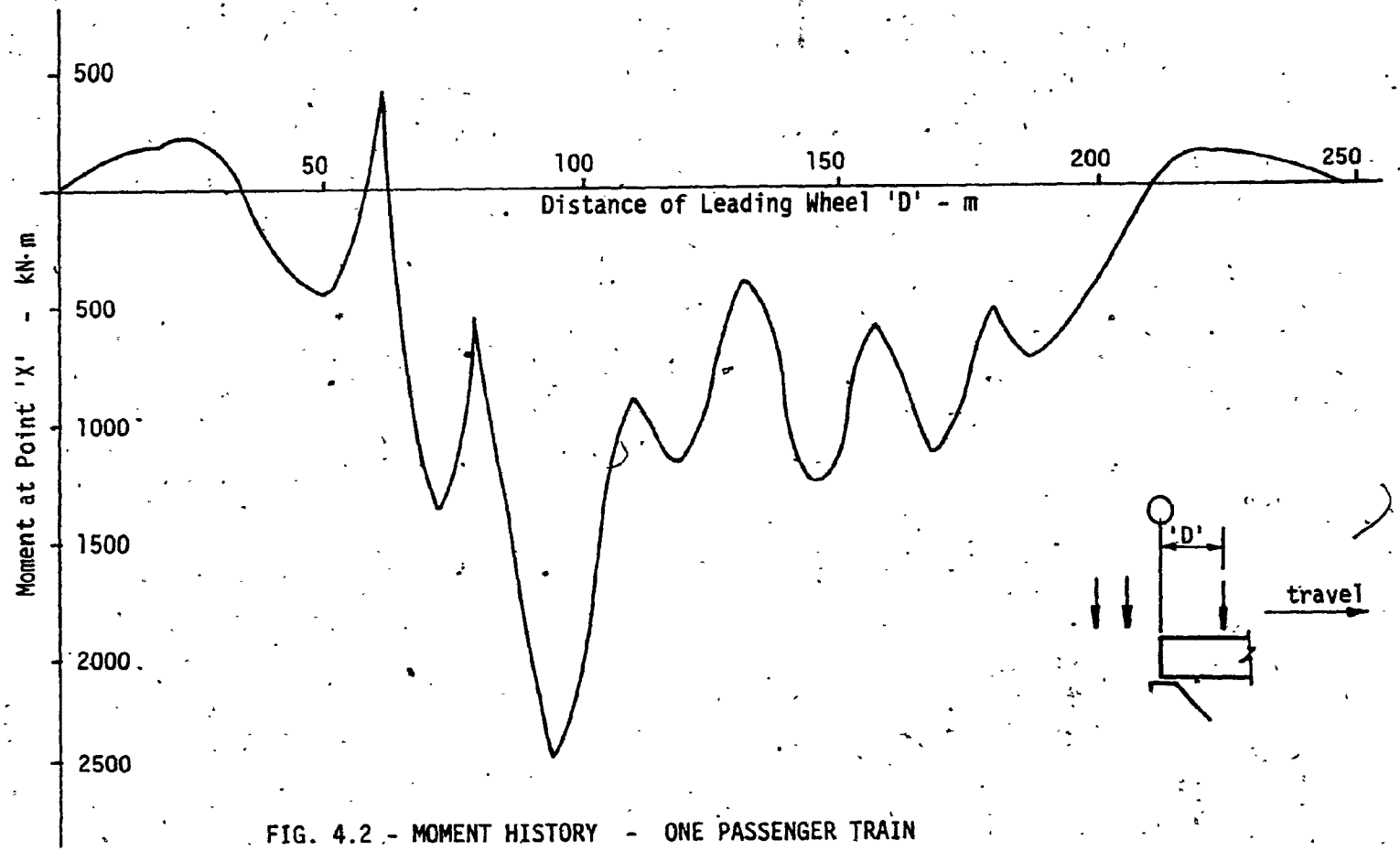

FIG. 4.2 - MOMENT HISTORY - ONE PASSENGER TRAIN

as a cross section of a reservoir which is successively drained from each low point, counting one cycle for each draining operation. The results are tabulated in descending order of magnitude in Table 4.1.

For reference the information used in the calculation of the moment ranges is included in Appendix 'B' consisting of the following:

1) influence line coefficients
2) method of calculating moments
3) cycle calculations using the "reservoir method"
4) summary of moment ranges.

MOMENT ID	MOMENT RANGE (per track)	NUMBER of CYCLES
	kN·m	
M1	2880	1
M2	854	1
M3	849	1
M7	673	1
M5	481	1
M4	279	1
M6	216	1
M8	167	1

TABLE 4.1 - MOMENT RANGES (ONE PASSENGER TRAIN)

4.3 Moment Range History - Freight Train

The moment range history spectrum of a freight train was derived from the information developed to compile the moment range history spectrum of a passenger train. The passenger train data was adjusted to account for the heavier loading as well as the greater number of freight cars. These adjustments are described in detail in Appendix B.3. The resulting moment history spectrum is plotted in Fig. 4.3.

Using the same method of cycle counting as for the passenger train, the results are tabulated in descending order of magnitude with the corresponding cycles in Table 4.2.

MOMENT ID	MOMENT RANGE (per track) kN m	NUMBER of CYCLES
M1	8189	1
M2	3203	1
M3	2511	45
M4	2511	1
M7	2061	1
M5	1931	1
M9	1599	1
M6	1132	1
M8	868	1
M10	343	1

TABLE 4.2 - MOMENT RANGES (ONE FREIGHT TRAIN).

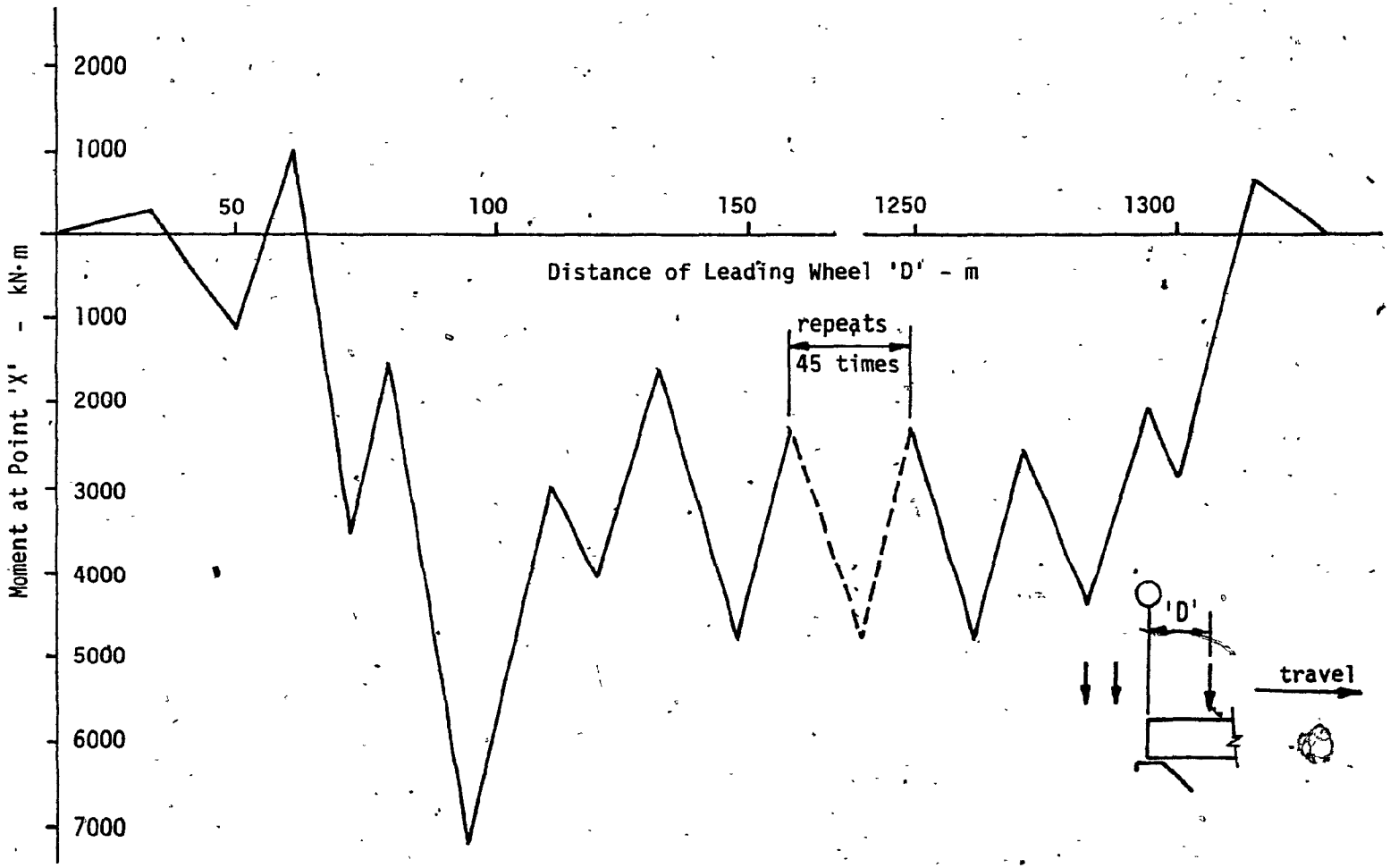

FIG. 4.3 - MOMENT HISTORY - ONE FREIGHT TRAIN

4.4 Impact Calculations

In addition to the live load moments, the effects of vertical impact and rolling impact must be added as both these effects amplify the range of stress the detail will experience during the passage of a live load.

Vertical Impact

CSA Standard S1 - 1950 'Steel Railway Bridges', requires that a "percentage of the static live load equal to

$$I_V = \frac{600}{(L - 30)} + 16 \qquad (4.1)$$

where: I_V = vertical impact percent

L = length in feet, centre-to-centre of supports

be added for the direct vertical effect of impact".

In the case of this bridge the vertical impact percent is:

$$I_V = \frac{600}{(117.5 - 30)} + 16$$

$$= 22.9\%$$

Rolling Impact

CSA S1 - 1950 also requires that "vertical forces due to the rolling of the train from side to side, acting downward on one rail and upward on the other, the forces on each rail being equal to 10 percent of the static live load per track" be added.

4.5 Design Moment Range Summary

The bridge girder is subjected to a number of fluctuating load effects from live load, vertical impact and rolling impact during the passage of both passenger train and freight train traffic. These effects, discussed in sections 4.2, 4.3, and 4.4, are summarized in Table 4.3 and sum up to give the 'Design Moment Range'.

4.6 Stiffener Stress Range Calculations

Using simple beam theory, the stress at the longitudinal horizontal stiffener can be calculated from the following formula:-

$$f = \frac{M\,y}{I} \qquad (4.2)$$

where: f = stress at the stiffener

M = moment at the failure location (Point 'X')

y = distance from the neutral axis of the girder to the stiffener

I = moment of inertia of the total girder section about its neutral axis

For reference, the detailed calculations of the moment of inertia are included in Appendix C.

By using the moment range from Table 4.3 in the above formula the resulting stress becomes the stress range which the horizontal stiffener is subjected to during the passage of the moving loads.

The summary of the stress ranges at the horizontal stiffener corresponding to the various moment ranges listed in Table 4.3 was

	MOMENT RANGE /track	MOMENT RANGE /girder	VERTICAL IMPACT	ROLLING IMPACT	DESIGN MOMENT RANGE	CYCLES /train
	kN·m	kN·m	kN·m	kN·m	kN·m	
Passenger Train	2880	1440	330	288	2058	1
	854	427	98	85	610	1
	849	425	97	85	607	1
	673	337	77	67	481	1
	481	241	55	48	344	1
	279	140	32	28	200	1
	216	108	25	22	155	1
	167	84	19	17	120	1
Freight Train	8189	4095	938	819	5852	1
	3203	1602	367	320	2289	1
	2511	1256	288	251	1795	45
	2511	1256	288	251	1795	1
	2061	1031	236	206	1473	1
	1931	966	221	193	1380	1
	1599	800	183	160	1143	1
	1132	566	130	113	809	1
	868	434	99	87	620	1
	343	172	39	34	245	1

TABLE 4.3 - DESIGN MOMENT RANGES

compiled and is shown in Table 4.4

DESIGN MOMENT RANGE	STRESS at STIFF.	CYCLES /train	DESIGN MOMENT RANGE	STRESS at STIFF.	CYCLES /train
kN·m	MPa		kN·m	MPa	
Passenger Train			Freight Train		
2058	15.09	1	5852	42.91	1
610	4.47	1	2289	16.79	1
607	4.45	1	1795	13.16	45
481	3.53	1	1795	13.16	1
344	2.52	1	1473	10.80	1
200	1.47	1	1380	10.12	1
155	1.14	1	1143	8.38	1
120	0.88	1	809	5.93	1
			620	4.55	1
			245	1.80	1

TABLE 4.4 - STIFFENER STRESS RANGES

4.7 Design Stress Range Calculations

Whenever the "line of stress" is deflected from a regular path, the stress increases at the deflection and this phenomenon is commonly referred to as the "stress concentration".

In the case of a partial penetration weld this stress

concentration has two factors that must be evaluated. First is the reduced section available to transmit the load which can be evaluated by using the net section available. Second and perhaps more severe is the stress concentration caused by the resulting geometrical discontinuity.

The combined effects of these two factors can be determined either by special analysis such as a finite element analysis where the detail is modelled to reflect the actual geometrical discontinuity or by the use of stress concentration factors published in a number of reference texts.

This report used the latter approach to show how such a problem can be evaluated without the need of highly sophisticated computer analysis.

4.7.1 Effect of Reduced Section

Calculation of the stress due to the reduced section can be made by simply using the net area at the section where the load is transferred. Since the total load being transferred remains constant then:

$$f_n \cdot w \cdot t_n = f_g \cdot w \cdot t_g \qquad (4.3)$$

where: f_n = stress on net area

f_g = stress on gross area

w = width of stiffener

t_n = net thickness through throat of weld

t_g = gross thickness of stiffener

Since the stress amplification is the ratio of $f_n \div f_g$, formula

4.3, can be rearranged to give the required information as follows:

$$SCF_{net} = \frac{f_n}{f_g} = \frac{t_g}{f_n}$$

In this case with t_g = 16 mm, and t_n = 5 mm, the stress concentration is:

$$SCF_{net} = \frac{16}{5}$$

$$= 3.2$$

4.7.2 Effect of Geometric Discontinuity

The stress concentration effects due to geometric discontinuities have been studied widely both analytically and experimentally. The results have been published and provide the means of evaluating this effect without the necessity of highly involved and complex finite element modelling and analysis.

Most of the reference works are based on the assumption that any hole, or crack, can be represented by an elliptical hole.

Based on many observations made in the assembly of sheared stiffener material, similar to the horizontal stiffeners on the bridge, the gap at the welded edge of the splice can be considered to have a 1 mm gap. This gap can be approximated by "an equivalent ellipse" with a minor axis of 2 mm. Using these assumptions, the geometric discontinuity of the partial penetration splice weld can be drawn as shown in Fig. 4.4.

For the analysis of an elliptical hole, R.E. Peterson's reference text "Stress Concentration Factors" [2] states that the stress

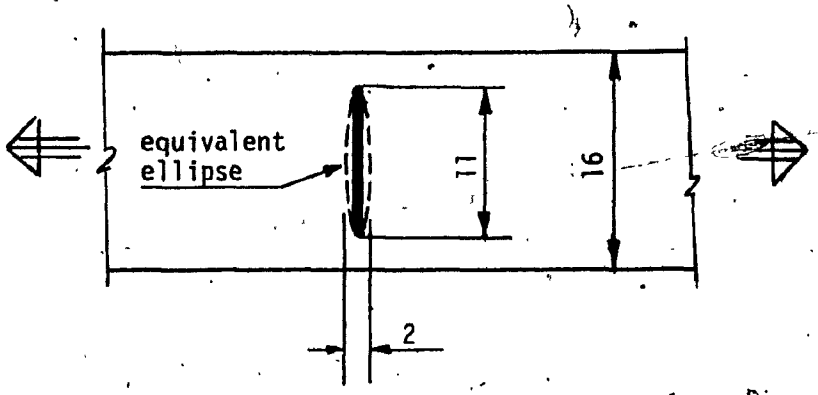

FIG. 4.4 - GEOMETRIC DISCONTINUITY ASSUMPTIONS

concentration factor, in an infinitely wide plate, was solved mathematically by Kolosoff [3] and Inglis [5], and is given by:

$$K_\infty = 1 + \frac{2b}{a} \qquad (4.4)$$

where: K_∞ = stress concentration factor in an infinitely wide plate

b = width of hole perpendicular to the applied stress

a = width of hole parallel to the applied stress

Formula 4.4 is shown in graphical form in Fig. 4.5.

Furthermore, for the very narrow ellipse, approaching a crack, a "finite-width correction" formula, developed by Koiter [6] can be used to adjust for the actual stiffener width in this case. The

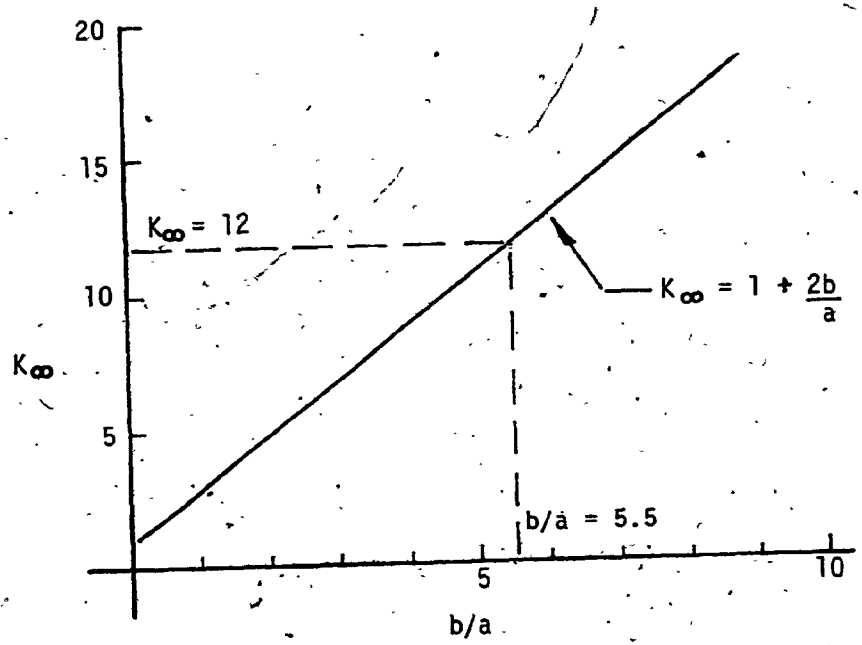

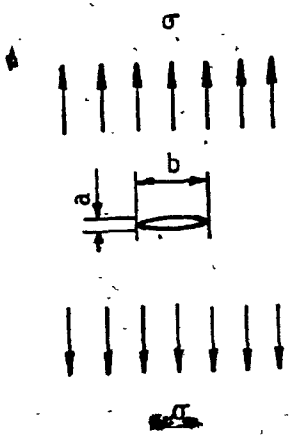

FIG. 4.5 – STRESS CONCENTRATION FACTOR, K_∞, for an ELLIPTICAL HOLE IN AN INFINITE PLATE

formula developed is the following:

$$\frac{K_{tn}}{K_{\infty}} = \left[1 - 0.5\frac{b}{w} + 0.326\left(\frac{b}{w}\right)^2\right]\left[1 - \frac{b}{w}\right]^{1/2} \qquad (4.5)$$

where: K_{tn} = stress concentration factor based on area stress

K_{∞} = stress concentration factor in an infinitely wide plate

b = width of hole perpendicular to the applied stress

w = width of the plate

Formula 4.5 is plotted as a graph in Fig. 4.6.

Using the detail information given in Fig. 4.4 where

$a = 2$ mm

$b = 11$ mm

$w = 16$ mm

the stress concentration in an infinitely wide plate is found, from Fig. 4.5 or Formula 4.4, for:

$b/a = 5.5$

$K_{\infty} = 12.0$

Furthermore the correction for a finite width is found from Fig. 4.6 or Formula 4.5, for:

$b/w = 0.69$

$K_{tn}/K_{\infty} = 0.45$

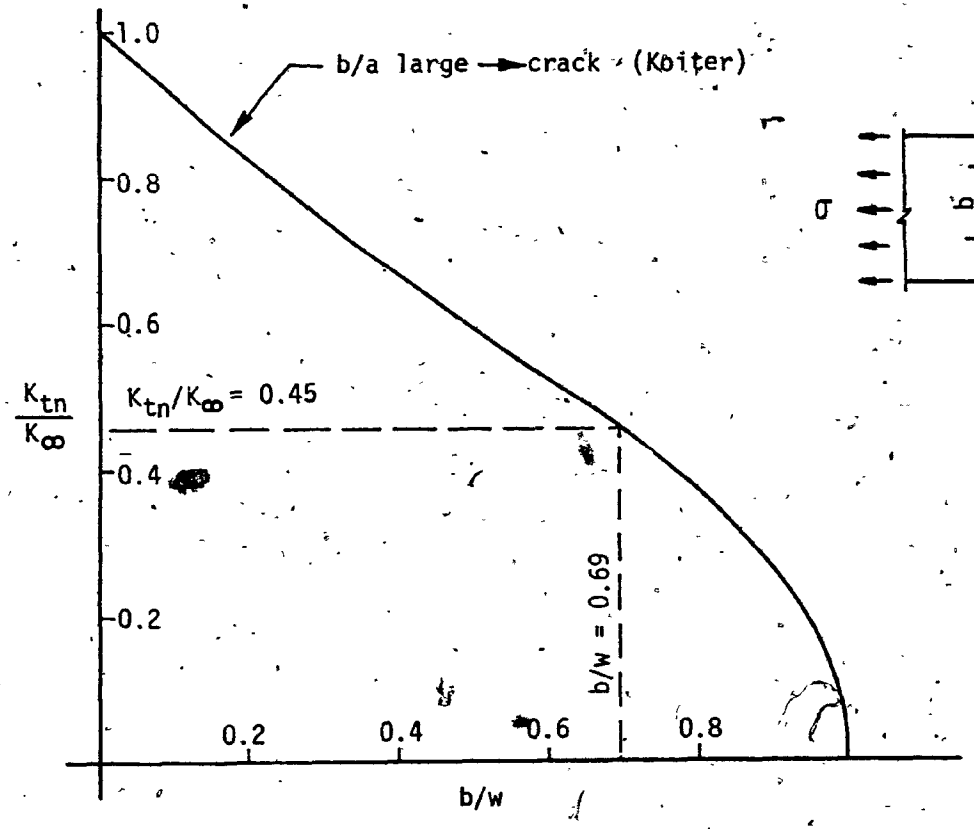

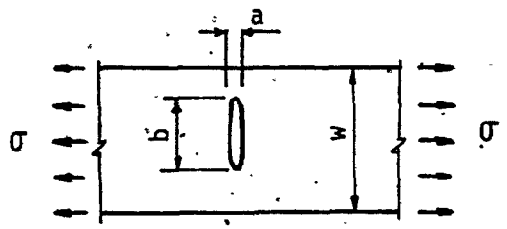

$K_{tn} = \sigma_{max} / \sigma_{nom}$

$\sigma_{nom} = \sigma / (1-b/w)$

$K_{t_\infty} = K_t$ for $w = \infty$

FIG. 4.6 - FINITE - WIDTH CORRECTION FACTOR, K_{tn}/K_∞

Combining the two, the stress concentration factor to be applied to the stress calculated on the net section, due to the geometric discontinuity, is calculated to be:-

$$K_{tn} = \frac{K_{tn}}{K_\infty} \times K_\infty$$
$$= 0.45 \times 12.0$$
$$= 5.4$$

4.7.3 Design Stress Range Summary

The design stress range to be used in calculating the fatigue life of the partial penetration weld is determined as the peak stress range that the detail is exposed to during the loading cycles. This is found by taking the stress range in the stiffener, adjusting for the effect of net section and multiplying the result by the stress concentration factor resulting from the geometric discontinuity.

This information, in summary form, is shown in Table 4.5 .

4.8 Fatigue Life Evaluation

Present day standards and supporting references provide information to calculate a fatigue life expectancy for many details. However, none of the various references reviewed deal specifically with partial penetration welded joints where the net weld throat specifically accounts for a very small percentage of the plate thickness. Most references provide data for the more usual type of weld where the net throat is 75% or more of the plate thickness. In our case

STIFFENER STRESS RANGE	STRESS * RANGE on NET SECTION	DESIGN # STRESS RANGE	CYCLES per train	STIFFENER STRESS RANGE	STRESS * RANGE on NET SECTION	DESIGN # STRESS RANGE	CYCLES per train
MPa	MPa	MPa		MPa	MPa	MPa	
Passenger Train				Freight Train			
15.09	48.29	260.8	1	42.91	137.31	741.5	1
4.47	14.30	77.2	1	16.79	53.73	290.1	1
4.45	14.24	76.9	1	13.16	42.11	227.4	45
3.53	11.30	61.0	1	13.16	42.11	227.4	1
2.52	8.60	43.5	1	10.80	34.56	186.6	1
1.47	4.70	25.4	1	10.12	32.38	174.9	1
1.14	3.65	19.7	1	8.38	26.82	144.8	1
0.88	2.82	15.2	1	5.93	18.98	102.5	1
				4.55	14.56	78.6	1
* - factor = 3.2 # - factor = 5.4				1.80	5.76	31.1	1

TABLE 4.5 - DESIGN STRESS RANGE and CYCLES

with the net throat comprising only 30% of the plate thickness, it was decided that the guidelines and information provided could not be used with any degree of confidence.

As a consequence the approach used follows the general guidelines of BS 5400 : Part 10 : 1980. The specific steps used were:

1. The design stress at the root face of the partial penetration weld was the stress on the net section multiplied by the stress concentration factor, as shown in Table 4.5

2. A joint classification was selected that was equivalent to a flame cut surface with similar geometric properties from BS : 5400 :1980 : Part 10.

3. The "cumulative damage calculations" outlined in BS : 5400 : Part 10 : 1980 Clause 11 and Appendix 'A' were used to calculate the life expectancy of the joint detail.

4.8.1 Joint Classification

Appendix 'H' - "Explanatory Notes on Detail Classification" in BS 5400 : Part 10 : 1980 states that "the stress concentrations inherent in the make-up of a welded joint have been taken into account in the classification of the detail. However, where there is a geometrical discontinuity, such as a change of cross section or an aperture, the resulting stress concentrations should be determined either by special analysis or by the use of the stress concentrations factors available".

In this case the usual classification for a partial penetration or fillet weld would be a Class W. However, since the Class W joint has some degree of stress concentration included in its design parameters and because the stress concentrations from the severe geometric discontinuity have been accounted for separately, the choice of Class W would result in overstating the stress concentration effects.

By comparing the critical corner of a cruciform joint with an enlarged view of the inside corner of the partial penetration weld, both shown circled in Fig. 4.7, the similarity become quite evident. Accordingly, a more rational selection is to classify the partial penetration weld as a Class F joint. For this classification BS 5400 : Part 10 : 1980 requires that stress concentration factors be included, which is consistent with the approach followed in this analysis.

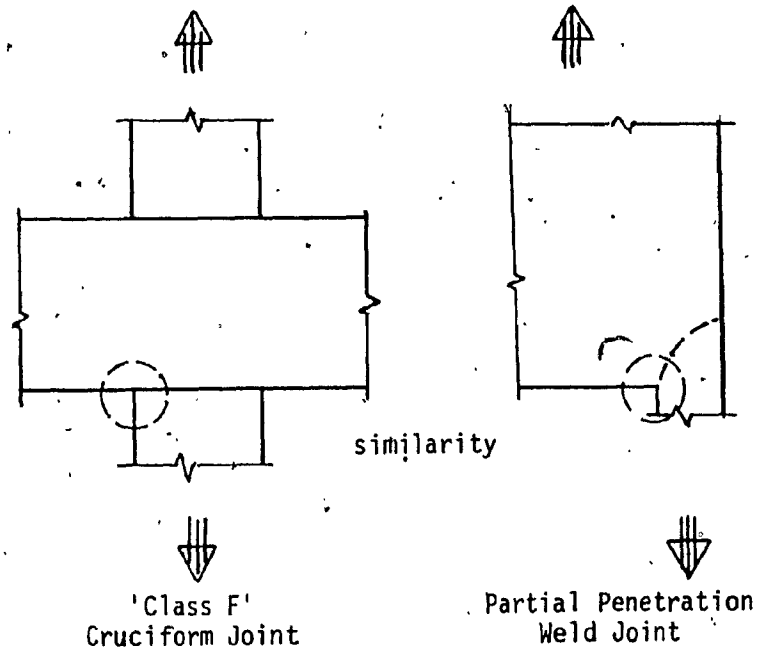

FIG. 4.7 - COMPARISON of JOINTS

4.8.2. Calculation of Non-Propagating Stress Range

When a detail is subjected to fluctuating stress of constant amplitude, there is a certain stress range below which an indefinitely large number of cycles can be sustained without failure. The value of this "non-propagating stress range" can be determined from the following equation, given in BS 5400 : Part 10 : 1980 Appendix 'A' ..

$$N \times \sigma_r^m = K_o \times \Delta^d \qquad (4.6)$$

where : N = the predicted number of cycles to failure of the stress range σ_r

K_o = the constant term relating to the mean line of the statistical analysis results

m = the inverse slope of the mean-line log σ_r - log N curve

Δ = the reciprocal of the anti-log of the standard deviation of log N

d = the number of standard deviations below the mean-line

For the joint being analysed the following values are appropriate:

d = 3.0 This value corresponds to a probability of failure of 0.14%. This value was chosen as the task is to evaluate an actual failure.

$N = 10^7$ This value is the accepted endurance limit

σ_o = This value corresponds to the non-

propagating stress range for $N = 10^7$

$K_o = 1.73 \times 10^{12}$
$\Delta = 0.605$
$m = 3.0$

These values correspond to values for a Class 'F' detail in BS 5400

Using Equation 4.6, the value of σ_o is calculated as follows:

$$N \times \sigma_o^m = K \times \Delta^d$$

$$\sigma_o^m = \frac{K \times \Delta^d}{N}$$

$$\sigma_o^3 = \frac{(1.73 \times 10^{12})\ (0.605)^3}{10^7}$$

$$= 3.83 \times 10^4$$

$$\sigma_o = 33.7 \text{ MPa}$$

4.8.3 Life Expectancy Calculations

The treatment of low stress cycles, those below the non-propagating stress range, σ_o, have been ignored in the past. However, recent research suggests this to be in error and recommendations have been included in BS 5400 : Part 10 : 1980, Appendix 'A' for evaluating this feature of fluctuating stress histories.

BS 5400 states -- "when the applied fluctuating stress has varying amplitude, so that some of the stress ranges are greater and some less than σ_o, the larger stress ranges will cause enlargement of the initial defect. This gradual enlargement reduces the value of the non-propagating stress range below σ_o. Thus, as time goes on, an increasing number of stress ranges below σ_o can themselves contribute

to the further enlargement of the defect. The final result is an earlier fatigue failure than could be predicted by assuming all stress ranges below σ_o are ineffective".

Following BS 5400, the life expectancy of the partial penetration stiffener weld is calculated as follows:

$$\text{Life} = \frac{1}{\sum\left(\frac{n}{N}\right)} \qquad (4.7)$$

where: $\frac{n}{N} = \frac{n}{10^7}\left(\frac{\sigma_r}{\sigma_o}\right)^m$ when $\sigma_r \geq \sigma_o$

$\frac{n}{N} = \frac{n}{10^7}\left(\frac{\sigma_r}{\sigma_o}\right)^{m+2}$ when $\sigma_r < \sigma_o$

Using the design stress range and cycles from Table 4.5, the average loading history from Table 2.1 and the non-propagating stress range, σ_o, calculated in Section 4.8.2, the values to be used in Equation 4.7 are:

n = from Table 4.5 and Table 2.1

$N = 10^7$

σ_r = from Table 4.5

σ_o = 33.7 MPa

m = 3.0

Table 4.6 is a summary of the calculations to determine the life expectancy of the detail being analysed. It should be noted that only stress ranges that result in a finite life are shown in the Table, and for reference the first stress range giving a $\sum(n/N) = 0.000$ is shown.

	σ_r	$(\sigma_r/\sigma_o)^3$	n per year	(n/N)
Passenger	260.8	463.8	1460	0.068
	77.2	12.0	1460	0.002
	76.9	11.9	1460	0.002
	61.0	5.9	1460	0.001
	43.5	2.2	1460	0.000
Freight	741.5	10652.3	12	0.013
	290.1	637.9	12	0.001
	227.4	307.2	540	0.017
	227.4	307.2	12	0.000
			$\sum$ (n/N) =	0.104
Life Expectancy = 9.6 years				

TABLE 4.6 - LIFE EXPECTANCY CALCULATIONS

4.9 Conclusions

Based on the information provided of four passenger trains per day, one emergency light freight train per month, and an assumed gap in the stiffener fit-up of 1 mm, the time required to initiate a crack in the partial penetration stiffener splice weld is calculated to be 9.6 years.

Recognizing that the crack, when finally noticed, was after about

10 years of service and since the crack had propagated through the total width of the horizontal stiffener weld and 1.25 m of web, the calculation of the life expectancy is in remarkable agreement with the actual service experienced.

However, while these results are exceptionally good, one cannot assume that such precision can be expected in all cases. The two critical assumptions that affect such calculations are:

a) a realistic loading history

b) an accurate representation of the defect.

While the first of the above assumptions can be assessed with a good degree of accuracy from records, the second can only be based on experience and close examination of similar details. Nevertheless, the calculations can be used to give a good indication of potential problem areas and details.

CHAPTER 5

PROGRESSIVE STAGES OF FAILURE

5.1 Introduction

The major failure analysed in Chapter 4 can be considered to have occurred in a number of distinct stages. This chapter describes the various stages from the initial crack formation through to the final stage that existed at the time the failure was discovered.

Since the fracture faces could not be examined it was difficult to clearly define where brittle fracture may have occurred. However, it is clear that brittle fracture would have occurred when the crack, initiated by fatigue, grew to a critical size.

The various stages are shown in Fig. 5.1 together with some description to show the general direction in which the crack progressed.

5.2 Stage I -- Crack Initiation

Stage I of the failure was the crack initiation at the outer tip of the stiffener weld as shown in Fig. 5.1 (a).

Both top and bottom partial penetration welds had cracks initiated after approximately 9 1/2 years, as determined from the analysis described in Chapter 4. Since the bridge has a skew, a certain degree of racking will occur, resulting in the bridge suffering some lateral deflection. This lateral deflection caused the stiffener tip to be stressed to a higher level than the portion adjacent to the web. As a

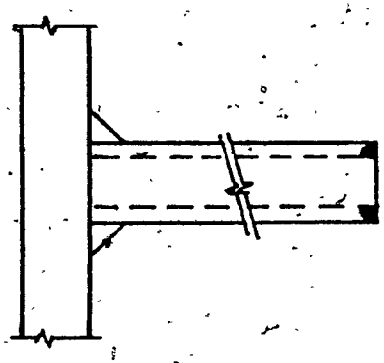

5.1 (a) - STAGE I

CRACK INITIATION

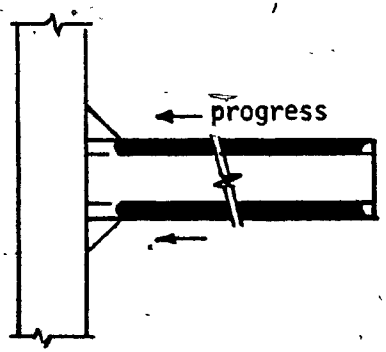

5.1 (b) - STAGE II

FAILURE - P.P. WELDS

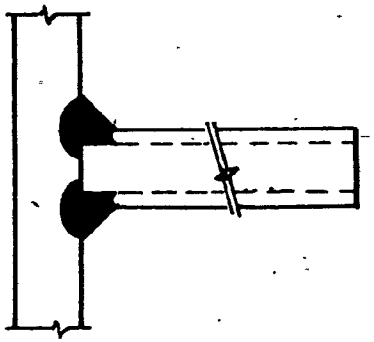

5.1 (c) - STAGE III

FAILURE - FILLET WELDS

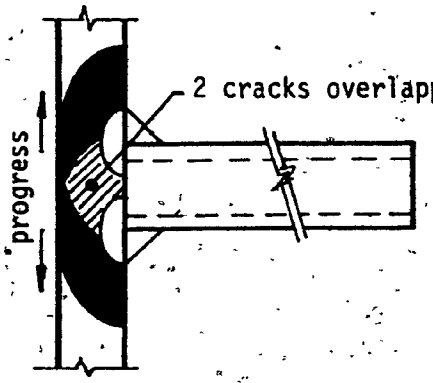

5.1 (d) - STAGE IV

FAILURE - WEB

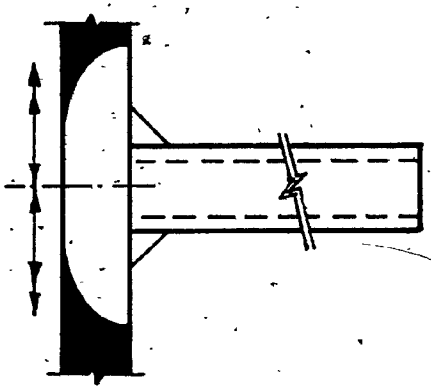

5.1 (e) - STAGE V

FINAL FRACTURE

FIG. 5.1

STAGES OF FAILURE

result the stiffener tip has a higher stress range and, therefore, it can be concluded that the crack would be initiated at that location.

5.3 Stage II -- Failure of P.P. Welds

Stage II of the failure consisted of the progressive failure of the partial penetration welds. The crack, initiated at the tip, progressed toward the stiffener to web fillet weld, as shown in Fig. 5.1 (b).

The initial progress was likely a classical fatigue failure, progressing in a ductile manner as additional loading cycles occurred. At some stage, the crack grew to a critical size and it is possible that a portion of the partial penetration welds failed in a brittle manner. This brittle fracture would require relatively little energy as the weld had little area.

At the stiffener to web fillet, however, there is a significant increase in weld area and the energy required to fail the partial penetration weld would be insufficient to drive the crack, in a brittle manner, through this much heavier weld. This would create the condition for the start of the next stage.

5.4 Stage III -- Failure of Fillet Welds

Stage III of the failure can be considered to have started when the cracks in the partial penetration welds penetrated the continuous horizontal fillet welds connecting the stiffener to the girder web.

The failure in the fillet welds was again a classical fatigue

failure driven by the loading cycles from both passenger and freight trains.

At this point the cracks started to turn from a vertical position, along the centre-line of the stiffener weld, to one normal to the direction of the principal stress. As a result the top crack and the bottom crack progressed in a slight lateral direction with respect to each other.

As the cracks progressed through the fillet weld, the crack tips also penetrated the web material at this stage and the final separation of the stiffener weld occurred.

The failure during this stage is shown in Fig. 5.1 (c).

5.5 Stage IV -- Failure of Web

Stage IV is a continuation of the failure through the main web material, as shown in Fig. 5.1 (d).

The top and bottom cracks progressed in classical fatigue fashion, driven by the periodic loading, at slightly different angles through the web with each following a direction normal to the principal stress at their respective location. As a result, two distinct and separate cracks continued to grow and, in fact, overlapped each other as shown in Fig. 5.1 (d). This resulted in a thin ligament of web separating the two cracks which provided the initial clue to the cause of the failure.

5.6 Stage V -- Final Fracture

Stage V is the total fracture, at the time the failure was discovered. This final stage is shown in cross-section in Fig. 5.1 (e). The web at that point was separated by two distinct cracks over a total length of 1.25 m. The upper crack was approximately 500 mm long and the bottom crack approximately 785 mm. The two cracks, each started at the horizontal stiffener and grew in opposite directions. At the horizontal stiffener, a thin ligament of web remained unbroken with the two cracks overlapping by approximately 60 mm.

Initially this stage was simply a continuation of the Stage IV failure. However, with the two cracks overlapping, the ends opposite each other created a flexible, bellows-like mechanism and further failure progress, at those ends, stopped. At the other ends the web material remained rigid and fatigue failure continued with each loading cycle.

It is probable that the last stages of the fracture failed in a brittle manner when the crack had grown to a critical size. The top end of the failure would have been arrested in a region of residual compression that resulted from the top flange to web welding, while the bottom end of the failure stopped near the neutral axis of the girder where the stress levels would be near zero or a net compression.

5.7 Probable Future Failure

Had the failure not been discovered the probable progress of the failure would have been the following:

1 - The bottom end of the failure, being near the neutral axis, where the stress range is very low, would have progressed slowly until it reached the neutral axis of the cracked section.

2 - The top end of the failure, being in a high net tension area, would have progressed more quickly and would have continued to propagate into the top flange.

3 - Having penetrated the top flange, the failure would have continued to grow until the remaining area of the top flange was insufficient to sustain the total load. At that point the top flange would have failed totally and the girder would attempt to carry the load as a simple span.

4 - With one half of the web already failed , the remaining portion of the web would be inadequate to carry the total shear load. It is probable that the span would have collapsed under the subsequent passage of a train.

CHAPTER 6

REPAIRS AND RETROFITTING

6.1 Introduction

The classical and most effective way of stopping a crack is to drill a round hole at the end of the crack. It is, however, critically important that the hole contains the crack tip. Careful inspection is required to ensure that the hole did, in fact, eliminate the crack tip.

The best method for retrofitting failures where material has become separated is to use a bolted splice, provided the location permits the drilling of holes and the installation of bolts.

This chapter describes the repair and retrofitting carried out on the following elements:

a) All horizontal stiffener welded splices, including those where no cracks were uncovered.

b) The girder web at the major failure where total separation of the web material occurred.

6.2 Repair and Retrofitting of Horizontal Stiffener Splices

At the three locations where cracks were found in the horizontal stiffener, a 38 mm diameter hole was drilled through the web from the inside face of the girder. The hole was centred to ensure that the total stiffener thickness and weld were contained within the hole

diameter. The drilling was continued for a distance of about 20 mm into the horizontal stiffener material.

After the drilling operation was completed, the hole was checked to ensure that no crack existed beyond the area that was drilled. This inspection was by means of dye penetrant, a procedure suitable for inspecting difficult to reach surfaces.

With the welded splice now isolated from the girder web, the horizontal stiffener weld was flame cut to separate the two sides of the stiffener splice. This procedure ensures that any crack in the partial penetration weld was removed totally.

Finally, the horizontal stiffener was re-spliced by means of a splice plate connected with high strength bolts.

Details of the total retrofitting scheme for the horizontal stiffener splice is shown in Fig. 6.1.

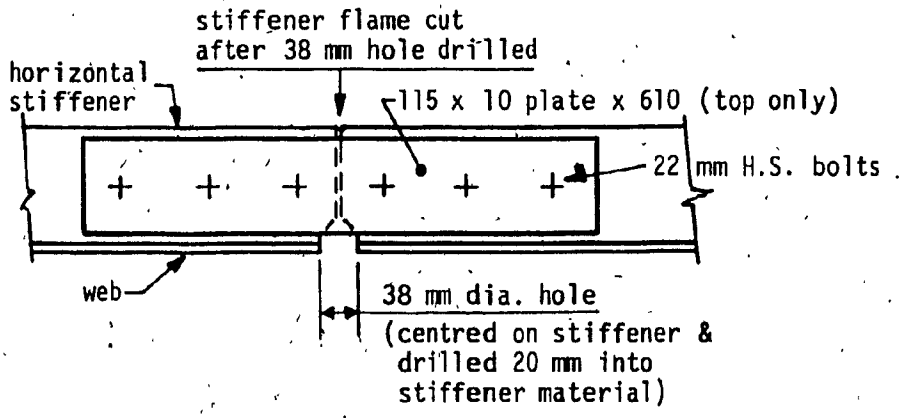

FIG. 6.1 - RETROFIT AT HORIZONTAL STIFFENER WELDED SPLICES

Having discovered cracks in the horizontal stiffener welded splices at three locations, it was concluded that all other horizontal stiffener splices were probably welded using the same procedure and therefore could develop similar cracks. To ensure that no future failure could originate in similar partial penetration welds, the identical procedure of retrofitting was carried out at the other 63 horizontal stiffener splice locations.

6.3 Repair and Retrofitting of Girder Web

To ensure that the existing crack in the girder web was arrested, a 25 mm diameter hole was drilled at each end of the two web cracks. In addition, the unbroken ligament of the web was cut through during the drilling for retrofitting of the horizontal stiffener, as described above in Section 6.2.

Again to ensure that the crack tips had been removed all the drilled holes were inspected with dye penetrant.

Retrofitting to replace the failed web capacity for shear and bending was accomplished by means of splice plates on both sides of the web, connected with 22 mm high-strength bolts. The bolt pattern was adjusted to provide acceptable edge distance along the crack location.

Details of the final web splice provided are shown in Fig. 6.2.

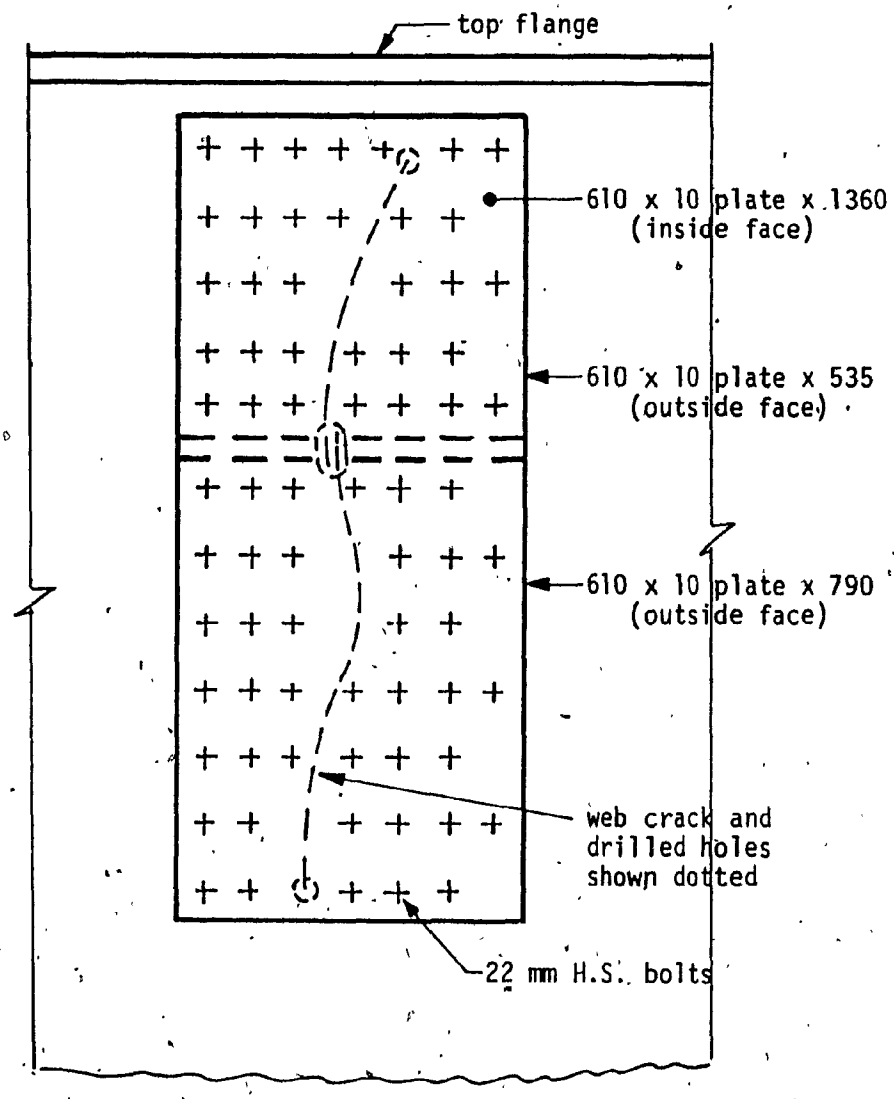

FIG. 6.2 - RETROFIT OF WEB FRACTURE

CHAPTER 7

INSPECTION OF RETROFITS

7.1 Introduction

In October 1985, nine years and four months after the failure had been retrofitted, a visual inspection was carried out by the writer to assess the suitability of the retrofits. Although no bolts nor splice plates were removed, a close examination was made at all the critical locations. Careful examinations were made of the holes drilled through the web which were left uncovered opposite the horizontal stiffener splice locations for evidence of new cracks. In addition a close look was taken at the bolted web splice plates for any evidence of slippage of the bolts.

7.2 Results of Inspection

Examination of the 62 uncovered holes drilled opposite the horizontal stiffener splices showed no evidence of new cracking. Further examination of the bolted splice in the horizontal stiffener showed no evidence of bolt slip nor any sign of cracking at the end of the weld connecting the horizontal stiffener to the girder web.

Examination of the bolted web splice plates showed no evidence of bolt slip, as the paint applied in 1976 had not cracked in the corner between the splice plates and the girder web. While it was impossible to confirm absolutely the effectiveness of the drilled holes in arresting the web cracks without removing the splice plates,

the fact that the retrofit showed no signs of distress for over nine years of service and that there was no evidence of paint cracking between the splice plate and the web, which would have likely occurred had further cracking taken place, tends to suggest that the drilled holes were effective in arresting the web cracks.

CHAPTER 8

CONCLUSIONS AND RECOMMENDATIONS

8.1 Introduction

Failures, inspite of the fact that they are undesirable, have very useful functions. First, they force the engineer to re-evaluate the design in an attempt to explain the reason or reasons for the failure. Second, this re-evaluation provides better insight into the functioning of the structure enabling improvements to be made to existing specifications. Third, they provide an opportunity to evaluate the manufacturing procedures used. Fourth, they provide an opportunity to evaluate the suitability of retrofitting procedures.

This chapter deals with the specific conclusions reached from the detailed analysis of the design and manufacturing procedure used, and recommendations are provided for future designs.

8.2 Conclusions

From the results of the study of this railway girder bridge failure the following specific conclusions can be drawn:

1.- The passage of a train, or vehicle, across a bridge generally produces a single major load cycle. In continuous bridges, however, the single passage of a train can cause multiple load cycles which must be accounted for in the fatigue evaluation.

2 - Members that are considered redundant in the initial design participate as part of the total structure in service and therefore can "pick up" significant stresses not anticipated in the original design.

3 - A crack can continue to propagate and even change direction under dynamic loading unless there is a void that can act as a crack arrestor.

4 - Partial penetration welds are difficult to evaluate, for fatigue performance, due to the ill-defined profile of the unfused area. This geometric discontinuity can result in extremely high stress concentration factors.

5 - The "Cumulative Damage" approach outlined in BS 5400 : Part 10 : 1980 provides a convenient method of evaluating the fatigue life of various details. Furthermore, the approach can be used on any structure as it accounts for multiple cycles, variable amplitude loading and the effects of low stress cycles.

6 - Drilled holes are effective in arresting cracks provided the total crack tip has been removed.

7 - High strength bolted splice plates are an effective and efficient means of retrofitting failures.

8.3 Recommendations

From the problems encountered in analysing the bridge failure

and developing solutions to provide a satisfactory retrofit, the following recommendations can be made:

1 - Specifications should recommend that multiple cycle loading from the passage of a single vehicle or train should be evaluated when checking for fatigue.

2 - Secondary members, that participate with main members in carrying load, must be treated as principal members when designing connection details.

3 - Intersecting welds should be avoided. This approach would prevent the build up of high residual stresses from the welding and in addition provide a natural crack arrestor in the connection detail.

4 - All welded splices should be shown on the shop detail drawings and be approved by the Design Engineer.

5 - All welded splices should have suitable non-destructive examination specified to ensure that defects, if present, are of an acceptable size.

6 - Design specifications should provide more guidance for the fatigue evaluation of multiple cycle, variable amplitude loading conditions.

REFERENCES

1. BS 5400 : PART 10 : 1980, "Code of Practice for Fatigue", British Standards Institution, London, England, 1980

2. PETERSON, R.E., "Stress Concentration Factors", John Wiley & Sons, New York, 1974

3. KOLOSOFF, G., "Disertation", St. Petersburg, 1910. (See Timoshenko, S., Ref. 4, p. 306.)

4. TIMOSHENKO, S., "Strength of Materials, Part II, 3rd. Ed.", Van Nostrand, Princeton, N.J., 1956

5. INGLIS, C.E., "Stresses in a Plate due to the Presence of Cracks and Sharp Corners", Engineering (London), Vol. 95, 1913, p.415.

6. KOITER, W.T., "Note on the Stress Intensity Factors for Sheet Strips with Crack under Tensile Loads", Report 314 of Laboratory of Engineering Mechanics, Technological University, Delft, Holland, 1965

7. FISHER, J.W., FRANK, K.H., HIRT, M.A., and McNAMEE, B.M., "Effects of Weldments on the Fatigue Strength of Steel Beams", NCHRP Report 102, Transportation Research Board, Washington, D.C., 1970

8. FISHER, J.W., PENSE, A.W., ROBERTS, R., "Evaluation of Fracture of Lafayette Street Bridge", Journal of the Structural

Division, A.S.C.E. Vol 103, No. ST 7, Proceedings Paper 13059, July 1977

9. FISHER, J.W., PENSE, A.W., HAUSAMMANN, H., IRWIN, G.R., "Quinnipiac River Bridge Cracking", Journal of the Structural Division, A.S.C.E. Vol 106, No. ST 4, Proceedings Paper 15343, April 1980

10. FISHER, J.W., ALBRECHT, P.A., YEN, B.T., KLINGERMAN, D.J., and McNAMEE, B.M., "Fatigue Strength of Steel Beams with Welded Stiffeners and Attachments", NCHRP Report 147, Transportation Research Board, Washington, D.C., 1974

11. FISHER, J.W., BARTHELEMY, B.M., MERTZ, D.R., and EDINGER, J.A., "Fatigue Behaviour of Full Scale Welded Bridge Attachments", NCHRP Report 227, Transportation Research Board, Washington, D.C., 1980

12. FISHER, J.W., HAUSAMMANN, H., SULLIVAN, M.D., and PENSE, A.W., "Detection and Repair of Fatigue Damage In Welded Highway Bridges", NCHRP Report 206, Transportation Research Board, Washington, D.C., 1979

13. FISHER, J.W., "Bridge Fatigue Guide, Details and Design", AISC, New York, 1977

14. FISHER, J.W., and YEN, B.T., "Fatigue Strength of Steel Members With Welded Details", Engineering Journal, 4Q, AISC, New York, 1977

15. FISHER, J.W., "Guide to 1974 AASHTO Fatigue Specifications", AISC, New York, 1974

16. FRANK, K.H., and FISHER, J.W., "Fatigue Strength of Fillet Welded Cruciform Joints", Journal of the Structural Division, ASCE, Vol 105 No. ST 9, Sept. 1979

17. ALBRECHT, P.A., and FISHER, J.W., "An Engineering Analysis of Crack Growth at Transverse Stiffeners", Publications IABSE, Vol. 35-I, 1975

18. ALBRECHT, P.A., and YAMADA, K., "Rapid Calculation of Stress Intensity Factors", Proceedings, ASCE, Vol. 103, No. ST 2, Feb. 1977

19. SCHILLING, C.G., KLIPPSTEIN, K.H., BARSOM, J.M., and BLAKE, G.T., "Fatigue of Welded Steel Bridge Members Under Variable Amplitude Loading", NCHRP Report 188, Transportation Research Board, Washington, D.C., 1978

20. CICCI, F., and CSAGOLY, P., "Assessment of the Fatigue Life Of a Steel Girder Bridge", Ontario Ministry Of Transportation and Communication, Research and Development Division, Report 192, Toronto, Ontario, Sept 1974

21. GURNEY, T.R., "Fatigue Design Rules For Welded Steel Joints", The Welding Institute Research Bulletin, Vol. 17, May 1976

22. GURNEY, T.R., "Influence Of Residual Stresses On Fatigue Strength Of Plates With Fillet Welded Attachments", British Welding Journal, June 1960

23. GURNEY, T.R., "Fatigue Tests On Butt And Fillet Welded Joints In Mild And High Tensile Strength Steels", British Welding Journal Vol. 9, No. 11, 1962

24. GURNEY, T.R., "Cumulative Damage Calculations In The Spectrum", The Welding Institute Members Report 2/1976/E, March 1976

25. GURNEY, T.R., "Cumulative Damage Calculations With The Proposed New Fatigue Design Rules", The Welding Institute Members Report 4/1976/E, March 1976

26. GURNEY, T.R., "Fatigue Of Welded Structures", Cambridge University Press, 2nd edition, Cambridge, England, 1979

27. GURNEY, T.R., "The New Fatigue Design Rules For Welded Joints And Their Background", Paper 25, Session 12, Conference On The New Code For The Design Of Steel Bridges, Cardiff, Wales, 1980

28. HALSE, W.I., "The Fatigue Assessment Of Bridges To BS 5400", The Welding Institute Members Report, 1981

29. COMEAU, M.P., and KULAK, G.L., "Fatigue Strength Of Welded Steel Elements", University of Alberta, Structural Engineering Report No. 79, 1979

30. IRWIN, G.R., "Analysis Of Stresses And Strains Near The End Of A Crack Traversing A Plate", Journal of Applied Mechanics, ASCE Vol. 24, 1957

31. MINER, M.A., "Cumulative Damage In Fatigue", Transactions, ASME, Vol. 67, 1945

32. NORRIS, S.N., "The Prediction Of Fatigue Lives Of Welded Web Attachments", M.S. Thesis, Lehigh University, 1979

33. ZETTLEMOYER, N., "Stress Concentrations And Fatigue Of Welded Details", Ph.D. Dissertation, Lehigh University, 1976

34. AMERICAN RAILWAY ENGINEERING ASSOCIATION, "Fatigue Failures In Railway Bridges", Proceedings, AREA, Vol. 54, 1953

35. AISC, "Moments, Shears and Reactions -- Continuous Highway Bridge Tables", AISC, New York 1959

36. CSA STANDARD S1 - 1950, "Steel Railway Bridges", Canadian Standards Association, Rexdale, Ontario, 1951

37. SWEENEY, R.A.P., "Some Examples Of Detection And Repair Of Fatigue Damage In Railway Bridge Members", Transportation Research Board Conference, Washington, D.C., 1978

38. OHBDC, "Ontario Highway Bridge Design Code - 1983", Ministry Of Transportation and Communication, Toronto, Ontario. 1983.

39. AASHTO, "Standard Specification For Highway Bridges", 13th Edition, American Association of State Highway and Transportation Officials, Washington, D.C., 1983.

APPENDIX 'A'

REVIEW OF OTHER CODES

A.1 Introduction

In preparation for the analysis to determine the expected life of partial penetration, horizontal stiffener weld a number of specifications were reviewed for guidance. The specifications reviewed were:

(a) CAN3 - S6 - M78 "Design Of Highway Bridges"
Canadian Standards Association

(b) Ontario Highway Bridge Design Code - 1983
Ministry of Transportation and Communication, Ontario

(c) AASHTO 13th Edition - 1983 "Standard Specification For Highway Bridges"
American Association of State Highway and Transportation Officials

(d) BS 5400 - 1980 "Steel, Concrete and Composite Bridges"
British Standard Institute

A.2 Treatment Of Fatigue Analysis

Fatigue analysis in both North America and Britain is treated, as a general rule, in a similar manner. Both have accepted the stress range concept and use Miner's cumulative damage as the basis for calculating the life expectancy of various catagories of details. However,

major differences do exist in the guidance provided for the handling of non-standard details and non-standard loadings.

A.2.1 North American Approach

The three North American specifications reviewd treat the design for fatigue in an identical manner except for the mass of vehicle to be used in the calculations. The procedure used is as follows:

(a) The fatigue loading is based on the design vehicle

(b) The number of cycles of maximum stress range to be considered in the analysis is selected, based on the type of road and the average daily truck traffic expected

(c) Details are divided into Catagories based on the severity, roughly corresponding to their stress concentration factors

(d) An allowable stress range is specified for each catagory of detail varying with the number of cycles expected during the life of the detail being considered

(e) The member or detail is designed so that the actual range of stress does not exceed the allowable fatigue stress range specified for the particular member or detail.

However, no guidance is provided in any of the three North American specifications on how to handle non-standard loadings or variable amplitude stress ranges. A further difficulty is encountered when trying to assess the remaining life of an existing detail. This problem becomes

even more difficult when the loading patterns change .

A.2.2 British Approach

The British Standard BS 5400 provides three methods for the fatigue assessment of details and thus provides the required guidance and flexibilty for handling most details and a variety of loadings.

A.2.2.1 Simplified Procedure

This method determines the limiting value of the maximum range of stress for a 120 year design life and can be used when the following conditions are satisfied:

(a) The detail class is in accordance with sketches shown in Table 17 of the standard

(b) The design life is 120 years

(c) The fatigue loading is the standard load spectrum

(d) The annual flow of traffic is in accordance with Table 1 of the standard

For this procedure the actual stress range calculated from the standard fatigue vehicle must not exceed the allowable stress range specified.

A.2.2.2 Damage Calculation - Single Vehicle Method

This method determines the fatigue life of the detail in question and may be used when the standard design life and/or the annual flow given in Table 1 of the standard is not applicable. It should only be used when the following conditions are satisfied:

(a) The detail class is in accordance with sketches shown in Table 17 of the standard but not class S which covers shear connectors in concrete

(b) The fatigue loading is the standard load spectrum

For this method the predicted fatigue life of the detail is calculated using the Palmgren-Miner rule for damage calculation and must be less than the specified design life for the detail to be acceptable.

A.2.2.3 Damage Calculations - Vehicle Spectrum Method

This method involves an explicit calculation of Miner's summation and may be used for any detail for which the σ - N relationship is known and for any known load or stress spectrum. For this method the stress spectrum can be derived by traversing each vehicle in the load spectrum across the structure. Using the resulting design spectrum the value of Miner's summation is calculated as outlined in Clause 11 of the standard and includes the effects of stress levels below the non-propagating stress level. This summation should not exceed 1.0 for the fatigue life of the detail to be acceptable.

A.3 Conclusions

It is evident from the above comparison that the North American standards can best be applied to new designs as they are based on a predetermined expected life with the detail subjected to stress cycles from a standard vehicle loading at a frequency determined by the type of road.

On the other hand, the British Standard provides much more flexibility. It can be used for the design of new structures for standard loadings by following the procedure outlined in Section A.2.2.1 or A.2.2.2 above, or for non-standard loading by following the procedure outlined in Section A.2.2.3 above.

Furthermore, the method can be used to evaluate the remaining life of any particular detail if the historical loading is known and the expected loading in the future can be determined.

For the problem inherent in this study the British Standard provided the guidance as well as the methodology for evaluating the expected life of the detail that suffered failure.

APPENDIX 'B'

MOMENT RANGE CALCULATIONS

B.1 Influence Line Coefficients

The influence line coefficients used for calculation of the moment at the failure location are tabulated in Table B.1. These coefficients are based on an 'N' ratio (interior span to exterion span) of 1.25, with each span divided into ten (10) equal segments, as described in the AISC "Moments, Shears and Reaction Tables" [35]. The graphical representation of these coefficients is shown in Table 4.1.

B.2 Method of Calculating Moments for One Passenger Train

The passenger train loading used for moment calculations is made up of one passenger locomotive followed by four passenger cars as shown in Fig. B.1.

The train is moved progressively such that the front wheels are positioned at each one-tenth span interval. For each position the moment was calculated by summing the moments of each individual load. The moment of each individual load was calculated using the following formula:

$$M = CPL \qquad B.1)$$

where: M = moment

unit load @	coeff. M/PL	unit load @	coeff. M/PL	unit load @	coeff. M/PL	unit load @	coeff. M/PL
A.0	0	B.0	0	C.0	0	D.0	0
.1	.0034	.1	-.0098	.1	-.0455	.1	.0090
.2	.0066	.2	-.0205	.2	-.0743	.2	.0162
.3	.0093	.3	-.0299	.3	-.0890	.3	.0201
.4	.0115	.4	-.0360	.4	-.0920	.4	.0216
.5	.0128	.5	-.0363	.5	-.0858	.5	.0211
.6	.0131	.6	-.0287	.6	-.0726	.6	.0189
.7	.0122	.7	-.0110	.7	-.0548	.7	.0154
.8	.0098	.8	.0191	.8	-.0355	.8	.0108
.9	.0058	.9	.0637	.9	-.0163	.9	.0056

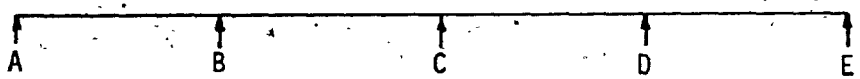

L = length of exterior span

NL = length of interior span

N = 1.25

TABLE B.1 - INFLUENCE LINE COEFFICIENTS

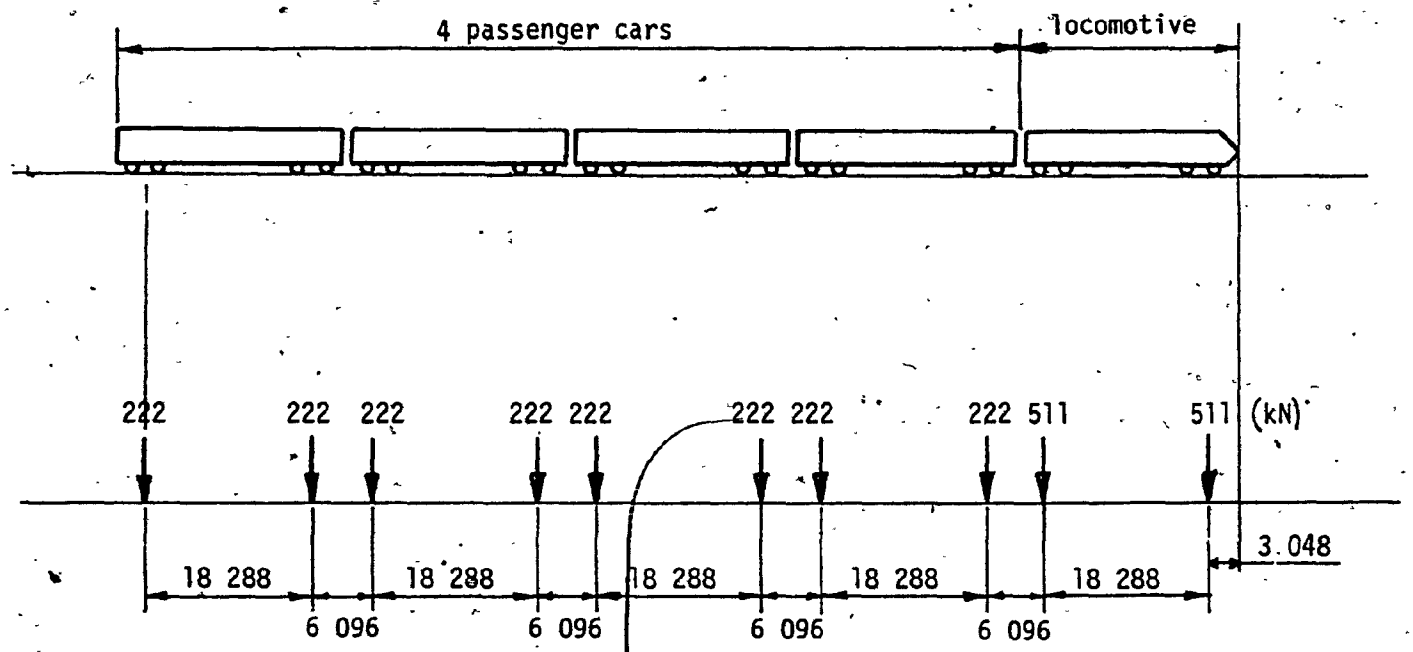

FIG. B.1 -- TYPICAL PASSENGER TRAIN LOADING

C = influence line coefficient (Table B.1)

P = corresponding point load

L = length of exterior span

Table B.2 lists the moments at the failure location corresponding to the position of the front wheel of the passenger train and is the data used to plot the moment history shown in Fig. 4.2.

B.3 Method of Calculating Moments for One Freight Train

The freight train loading used to develop the moment history is made up of one freight locomotive followed by fifty (50) freight cars as shown in Fig. B.2.

The moments were derived from the peak moments calculated for the passenger train crossing, shown in Table B.2, with adjustments made to account for the heavier loading and a greater number of cars. These adjustments were as follows:

1. From the start, position A.0, to position A.8 the moments were adjusted by the ratio of the freight locomotive load to the passenger locomotive load, a factor of 1.54.

2. Beyond position E50 the moments were adjusted by the ratio of the freight car load to the passenger car load, a factor of 4.0.

3. Between position A.8 and E50 the moments were adjusted progressively by a factor of between 1.54 and 4.0. This progressively larger adjustment accounted for the fact that as more freight cars filled the bridge the factor had to increase to bridge the

Front Wheel @	Moment kN·m	Front Wheel @	Moment kN·m	Front Wheel @	Moment kN·m	Front Wheel @	Moment kN·m	Front Wheel @	Moment kN·m	Front Wheel @	Moment kN·m
A.0	0	B.4	- 335	C.8	- 2450	20	- 589	160	- 516	300	155
A.1	50	B.5	- 424	C.9	- 2273	30	- 979	170	- 664	310	156
A.2	96	B.6	- 450	D.0	- 1814	40	- 1214	180	- 732	320	134
A.3	137	B.7	- 353	D.1	- 1275	50	- 1279	190	- 711	330	134
A.4	168	B.8	- 80	D.2	- 1124	60	- 1200	200	- 644	340	125
A.5	187	B.9	430	D.3	- 903	70	- 979	210	- 559	350	103
A.6	193	C.0	- 578	D.4	- 1016	80	- 636	220	- 468	360	73
A.7	198	C.1	- 1203	D.5	- 1159	90	- 626	230	- 344	370	38
A.8	223	C.2	- 1406	D.6	- 1182	100	- 670	240	- 239	380	0
A.9	217	C.3	- 523	D.7	- 1078	110	- 972	250	- 103		
B.0	187	C.4	- 552	D.8	- 887	120	- 1117	260	5		
B.1	159	C.5	- 1108	D.9	- 594	130	- 1102	270	89		
B.2	- 38	C.6	- 1569	E.0	- 430	140	- 964	280	146		
B.3	- 191	C.7	- 2179	10	- 472	150	- 671	290	167		

TABLE B.2 - MOMENT HISTORY at FAILURE LOCATION (One Passenger Train)

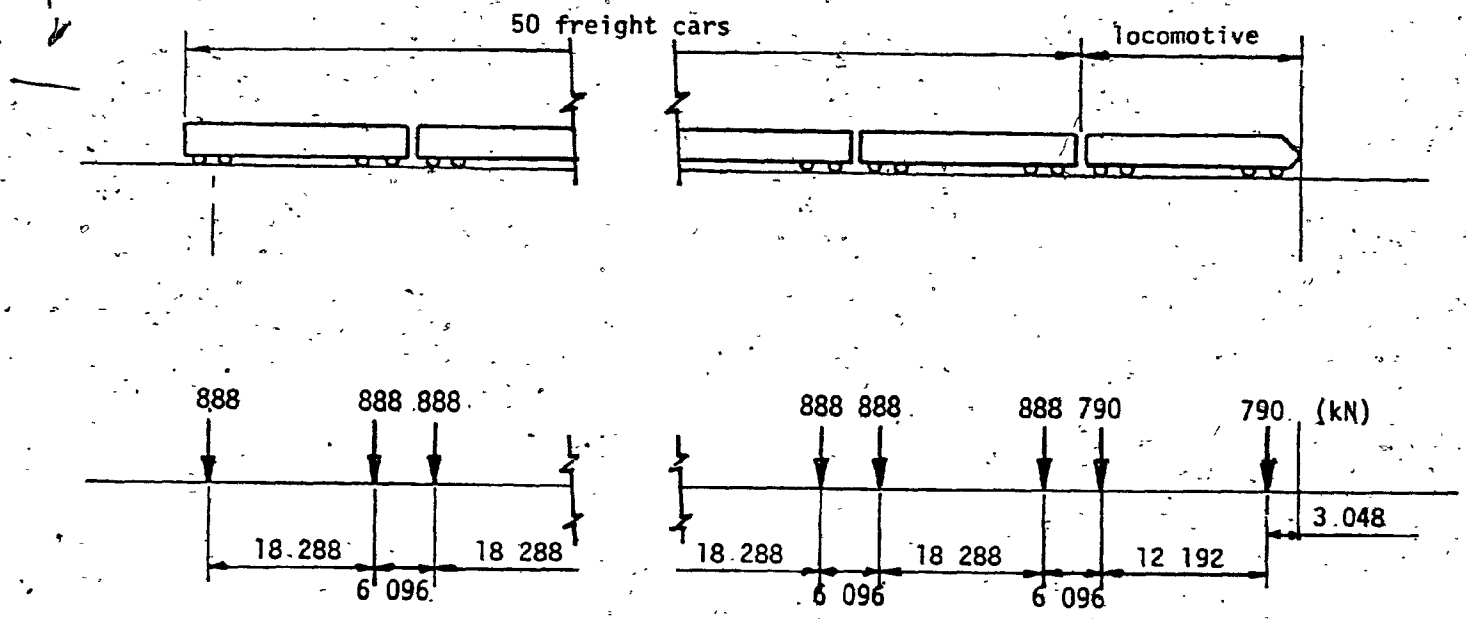

FIG. B.2 -- TYPICAL FREIGHT TRAIN LOADING

boundary conditions of Items 1 and 2, listed above.

4. Position E50 had a further adjustment of +324 kN·m to account for the additional front wheel load of a freight car required to fully load the bridge

5. Position E80 had an adjustment of +264 kN·m to account for one additional freight car to fully load the bridge.

6. Positions E50 and E80 are repeated forty five (45) times to account for the fifty (50) freight car train.

7. The final E50-46 and E80-46 positions are adjusted for the ratio of the freight car load to the passenger car load, or a factor of 4.0

Table B.3 lists the moments corresponding to the position of the front wheel of the freight train for the peak moment locations only and includes the adove adjustments. This data was used to plot the moment history shown in Fig. 4.3.

B.4 Cycle Counting By The 'Reservoir Method'.

The purpose of cycle counting is to reduce an irregular series of stress fluctuations to a simple list of stress ranges. The method is described in detail in BS 5400 : Part 10: 1980 as follows:

1. Derive the peak and trough values of the stress history, due to one loading event. Sketch the history due to two successive occurrences of this loading event. Mark the highest peak stress in

Front Wheel @	Passenger Train Moment kN·m	Adj. Factor	Adj. Moment kN m	Freight Train Moment kN·m	Front Wheel @	Passenger Train Moment kN·m	Adj. Factor	Adj. Momnet kN m	Freight Train Moment kN·m
A.0	0	0		0	E80-0	- 636	4.0	264	- 2280
A.8	223	1.54		343	E50-45	- 1279	4.0	324	- 4791
B.6	- 450	2.07		- 932	E80-45	- 636	4.0	264	- 2280
B.9	430	2.29		985	E50-46	- 1279	4.0	324	- 4791
C.2	- 1406	2.51		- 3529	E80-46	- 636	4.0		- 2540
C.4	- 552	2.66		- 1468	E120	- 1117	4.0		- 4471
C.8	- 2450	2.94		- 7204	E160	- 516	4.0		- 2062
D.3	- 903	3.25		- 2935	E180	- 732	4.0		- 2930
D.6	- 1182	3.69		- 4067	E290	167	4.0		668
E.0	- 430	4.0		- 1588	E380	0	0		0
E50-0	- 1279	4.0	324	- 4791					

TABLE B.3 - MOMENT HISTORY at FAILURE LOCATION (One Freight Train)

each occurrence.

2. Join the two marked points and consider only that part of the plot which falls below this line.

3. Drain the reservoir from the lowest point leaving the water that cannot escape. If there are two or more equal lowest points the drainage may be from any one of them. List one cycle having a stress range σ_r equal to the vertical height of water drained.

4. Repeat step (3) successively with each remaining body of water until the whole reservoir is emptied, listing one cycle at each draining operation.

5. Compile the final list which contains all the individual stress ranges in descending order of magnitude. Where two or more cycles of equal stress range are recorded, they can be listed separately or combined. If they are combined care should be taken to record the correct number of cycles corresponding to the particular stress range.

The above method is adaptable to any irregular series of fluctuations. In this case the fluctuations are, in fact, moment fluctuations and therefore the results are moment ranges.

Fig. B.3 shows graphically the procedure for the passenger train while Fig. B.4 shows the procedure for the freight train.

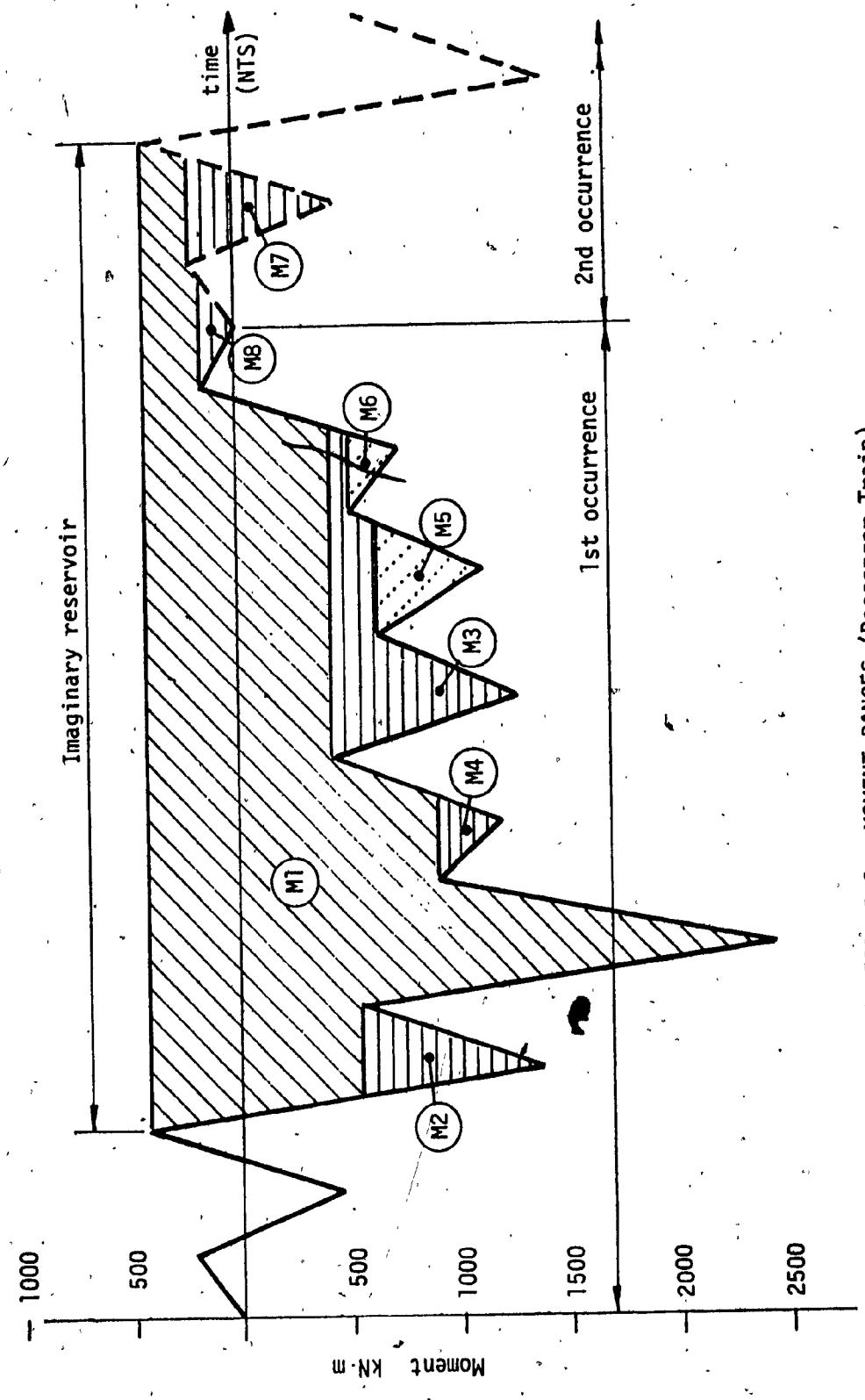

FIG. B.3 - MOMENT RANGES (Passenger Train)

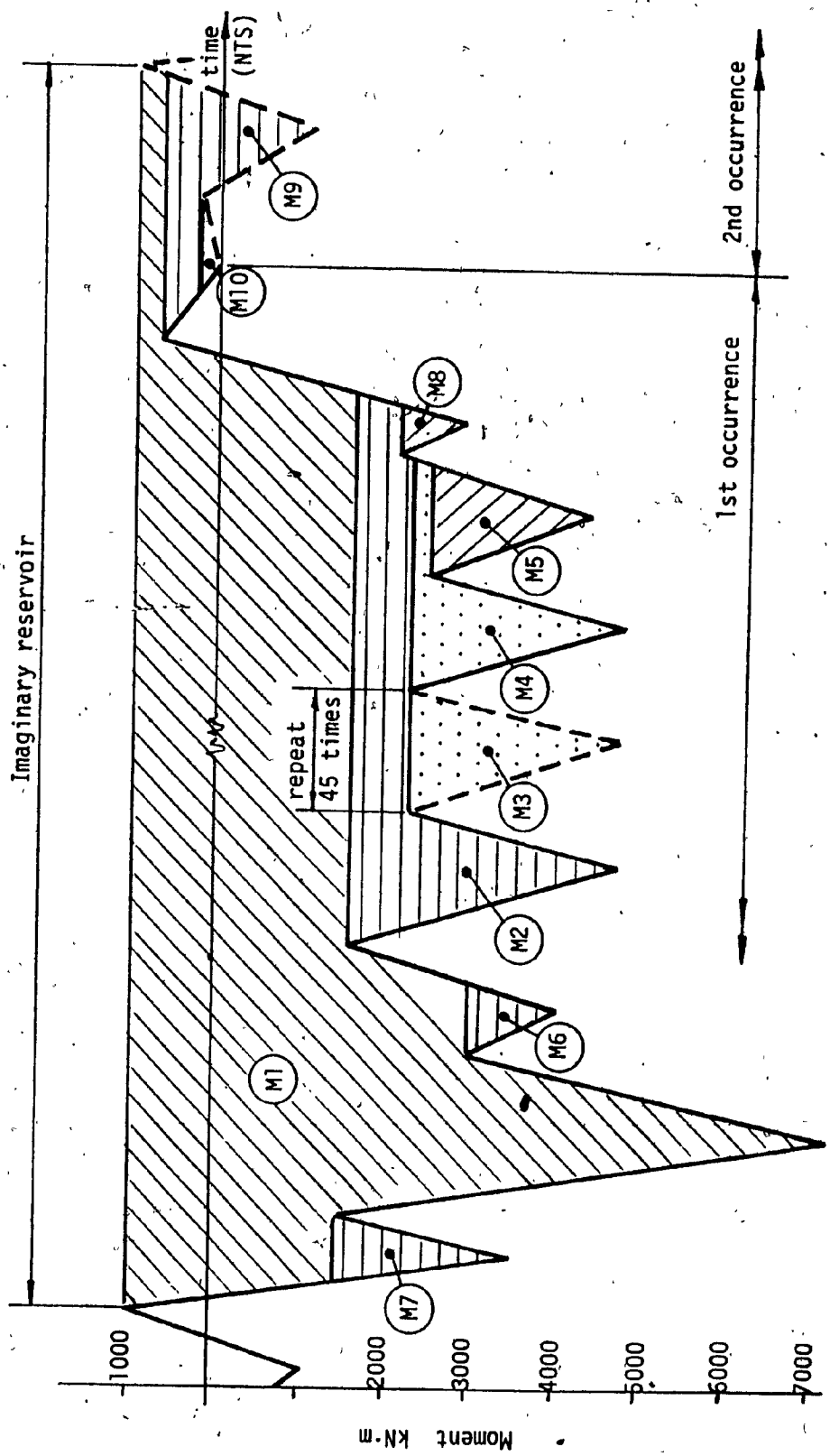

FIG. B.4 - MOMENT RANGES (Freight Train)

B.5 Summary of Moment Ranges

The moment ranges, for the passenger train, are calculated from Fig. B.3 and are shown in Table B.4. Similarly the moment ranges for the freight train are calculated from Fig. B.4 and are shown in Table B.5

Moment ID	Minimum - Maximum	Moment Range	Cycles
	kN·m	kN·m	
M1	- 2450 - 430	2880	1
M2	- 1406 + 552	854	1
M3	- 1279 + 430	849	1
M4	- 1182 + 903	279	1
M5	- 1117 + 636	481	1
M6	- 732 + 516	216	1
M7	- 450 - 223	673	1
M8	0 - 167	167	1

TABLE B.4 - MOMENT RANGES (One Passenger Train)

Moment ID	Minimum - Maximum	Moment Range	Cycles
	kN m	kN m	
M1	- 7204 - 985	8189	1
M2	- 4791 + 1588	3203	1
M3	- 4791 + 2280	2511	45
M4	- 4791 + 2280	2511	1
M5	- 4471 + 2540	1931	1
M6	- 4067 + 2935	1132	1
M7	- 3529 - 1468	2061	1
M8	- 2930 + 2062	868	1
M9	- 932 - 667	1599	1
M10	- 0 - 343	343	1

TABLE B.5 - MOMENT RANGES (One Freight Train)

APPENDIX 'C'

MOMENT OF INERTIA CALCULATIONS

The moment of inertia of a built up girder section can be calculated using the following formlua:

$$I = \sum_i (I_{xx} + Ay^2) \qquad (C.1)$$

where: I = moment of inertia of the total section about its neutral axis

I_{xx} = moment of inertia of an element about its own neutral axis

A = area of the element

y = distance from the total section neutral axis to the neutral axis of the element

The data for the girder being investigated, with the material sizes, is shown in Fig. C.1 while the calculation of the moment of inertia is shown in Table C.1.

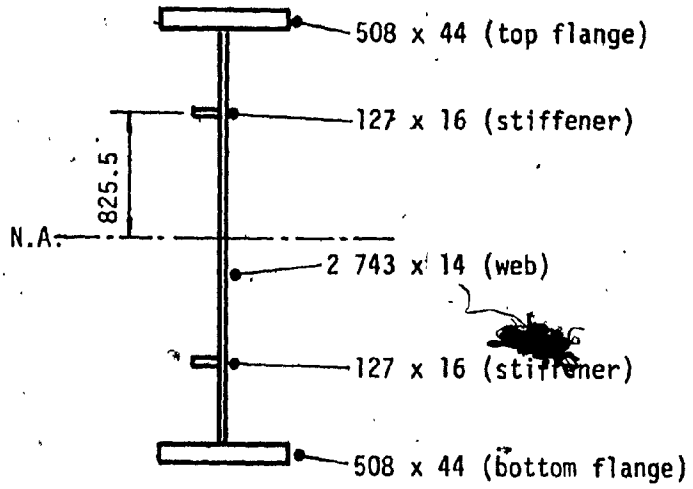

FIG. C.1 - GIRDER CROSS SECTION

Element	Area mm^2	I_{xx} $x10^6$ mm^4	y mm	Ay^2 $x10^6$ mm^4
508 x 44	22 352	4	1 393.5	43 404
127 x 16	2 032	0	825.5	1 385
2 743 x 14	38 402	24 078	0	0
127 x 16	2 032	0	825.5	1 385
508 x 44	22 352	4	1 393.5	43 404
		24 086		89 578
		I = 113 664 x 10^6 mm^4		

TABLE C.1 - MOMENT OF INERTIA CALCULATIONS